

Supporting Information for: Radiometallation and Photo-triggered Release of Ready-to-Inject Radiopharmaceuticals from the Solid Phase.

Table of Contents

Abbreviations	3
1. Experimental procedures	5
1.1 Materials	5
1.2 General Methods of Characterization	5
1.3 Photoreactor	5
2. Synthesis and Characterization of Peptides.....	7
2.1 Synthesis of BBN	7
2.2 Synthesis of PSMA	7
2.3 BBN deprotection	8
2.4 Quantitation of loading efficiency, deprotection and terminal cleavage	9
2.5 Photocleavage	13
2.6 Synthesis of ligands	13
2.7 HRMS, MALDI and HPLC characterization data	16
3. Synthesis and Characterization of Coordination Complexes.....	27
3.1 General Complexation Protocol.....	27
3.2 HRMS, MALDI and HPLC data of Coordination complexes.....	29
4. NMR data.....	35
5. Synthesis and Characterization of Radiochemical Complexes.....	42
5.1 General radiolabeling protocol	43
5.1.1 Resin preparation.....	43
5.1.2 Radiolabeling with ⁶⁷Ga.....	43
5.1.3 Radiolabeling with ⁶⁴Cu.....	43
5.1.4 Radiolabeling with ⁶⁸Ga.....	43
5.2 Synthesis of ⁶⁷Ga-radiolabeled complexes	44
5.2.1 Representative radiolabeling traces of NOTA-Aca-BBN (19).....	47
5.2.2 Representative radiolabeling traces of NOTA-PSMA (31).....	48
5.2.3 Concentration-dependent Radiolabeling.....	48
5.2.4 Volume-dependent radiolabeling	49
5.3 Synthesis of ⁶⁴Cu-radiolabeled complexes	51
5.3.1 Representative radiolabeling traces of NOTA-Aca-BBN (19).....	53
5.4 Synthesis of ⁶⁸Ga-radiolabeled complex	55
6. Tabulated data.....	58
7. References	63

Abbreviations

AA	Amino acid
Ac	Acetate
Aca	Aminocaproic acid
ADPA	Adipic acid
Anp	3-amino-3-(2-nitrophenyl)propionic acid
Boc	Tert-butyloxycarbonyl
Ci	Curie
DCM	Dichloromethane
DIEA	N,N-diisopropylethylamine
DMF	Dimethylformamide
DMSO	Dimethyl sulfoxide
DPBS	Dulbecco's phosphate buffered saline
EDC	1-Ethyl-3-(3-dimethylaminopropyl)carbodiimide
EDT	1,2-ethanedithiol
ESI-MS	Electrospray ionization mass spectrometry
Et ₂ O	Diethyl ether
FDA	Food and Drug Administration
Fmoc	fluorenylmethoxycarbonyl
Fmoc-6-Ahx-OH	6-(Fmoc-amino)hexanoic acid
HPLC	High performance liquid chromatography
ICP-OES	Inductively coupled plasma - optical emission spectrometry
LED	Light-emitting diode
MALDI	Matrix assisted laser desorption/ionization
MBq	Megabecquerels
MeCN	Acetonitrile
MeOH	Methanol
Mtt	4-Methyltrityl
Nap	Naphthyl
NHS	N-Hydroxysuccinimide

NOTA	1,4,7-Triazacyclononane-1,4,7-triacetic acid
PyBOP	(Benzotriazol-1-yloxy)tripyrrolidinophosphonium hexafluorophosphate
R _t	Retention time
SPPS	Solid-phase peptide synthesis
tBu	Tert-butyl
TG	Tentagel
TFA	Trifluoroacetic acid
TIS	Triisopropylsilane
WA	Wang resin

Amino acids are abbreviated using their conventional 3-letter codes.

1. Experimental procedures

1.1 Materials

All starting materials were purchased from Acros Organics, Alfa Aesar, Millipore Sigma or TCI America and used without further purification. Fmoc-protected amino acids were purchased from Bachem. NOTA-bis(t-Bu ester) compound was obtained from Macrocyclics. Agarose beads, amine functionalized, were purchased from NANOCS company. AmberLite® FPA66 Anion Exchange Resin free base and TentaGel™ S-NH₂ resins were purchased from Millipore Sigma. ⁶⁷Ga-citrate was received from Jubilant Radiopharma. ⁶⁴CuCl₂ isotope was produced and received from the University of Wisconsin, Medical Physics Dept., Madison, WI. ⁶⁸GaCl₃ was obtained from a ⁶⁸Ge/⁶⁸Ga generator (Eckhard & Ziegler, 30 mCi).

1.2 General Methods of Characterization

Mass spectrometry: High-resolution ESI mass spectrometry was carried out at the Stony Brook University Center for Advanced Study of Drug Action (CASDA) mass spectrometry facility with an Agilent LC-UV-TOF spectrometer. MALDI-TOF MS and high-resolution (ESI) mass spectrometry was carried out at the Stony Brook University Institute for Chemical Biology and Drug Discovery (ICB&DD) Mass Spectrometry Facility with an Agilent LC/MSD and Agilent LC-UV-TOF spectrometers, respectively. **NMR spectra** (¹H, ¹³C) were collected on a 700 MHz Advance III Bruker, 500 MHz, or 400 MHz Bruker instrument at 25 °C and processed using TopSpin 4.0.7. Chemical shifts are reported as parts per million (ppm). **Inductively coupled plasma spectroscopy (ICP)** was performed on an Agilent Technologies ICP-OES (Model 5110). A 10-point standard with respect to gallium or copper was used and lines of best fit were found with R² of 0.999. **UV-vis** spectra were collected with a NanoDrop 1 C instrument (AZY1706045). **High-Performance Liquid Chromatography (HPLC):** Semi-Preparative HPLC was carried out using a Shimadzu HPLC-20AR equipped with a binary gradient, pump, UV-vis detector, and manual injector on a Phenomenex Luna C18 column (250 mm × 21.2 mm, 100 Å, AXIA packed). Method A (Preparative Purification Method). A = 0.1% TFA in water, B = 0.1% TFA in MeCN. Gradient: 0-5 min: 95% A; 5-24 min: 5-95% B gradient. Analytical HPLC analysis was carried out using a Shimadzu HPLC-20AR equipped with a binary gradient, pump, UV-vis detector, autoinjector, and Laura radio-detector on a Phenomenex Luna C18 column (150 mm × 3 mm, 100 Å). Method B (Analytical HPLC analysis). A = 0.1% TFA in water, B = 0.1% TFA in MeCN with a flow rate of 0.8 mL/min, UV detection at 220 and 270 nm. Gradient 0-2 min: 5% B; 2-14 min 5-95% B; 14-16 min 95% B; 16-16.5 min 95-5% B; 16.5-20 min 5% B. Radio-HPLC analysis was carried out using a Shimadzu HPLC-20AR equipped with a binary gradient, pump, UV-vis detector, autoinjector, and Laura radio-detector on a Phenomenex Luna C18 column (150 mm × 3 mm, 100 Å). Method C (Radioanalysis). A = 0.1% TFA in water, B = 0.1% TFA in MeCN with a flow rate of 0.8 mL/min. Gradient 0-2 min: 5% B; 2-14 min 5-95% B; 14-16 min 95% B; 16-16.5 min 95-5% B; 16.5-20 min 5% B.

1.3 Photoreactor

The photoreactor device was constructed in accordance with previously published work¹ and adapted to hold syringes with resin in a supine position at variable distance from the LED light

source (<https://github.com/uw-madison-chem-shops/wisconsin-photoreactor>). The device consists of a base, reaction module and reactor driver (**Figure S1**). The base houses the photon source (365 nm LED) and cooling fan. The reaction module is comprised of a reflective reaction chamber and rigid syringe holder. A digital driver board integrating a commercial light-emitting diode (LED) driver is fitted to the base to drive the reactor. All 3D modules and size-variant syringe holders (**Figure S1**) were printed using a Original Prusa i3 MK3 3D printer. LED manufacturer is Inolux and manufacturer part number is IN-C39CTOU2.

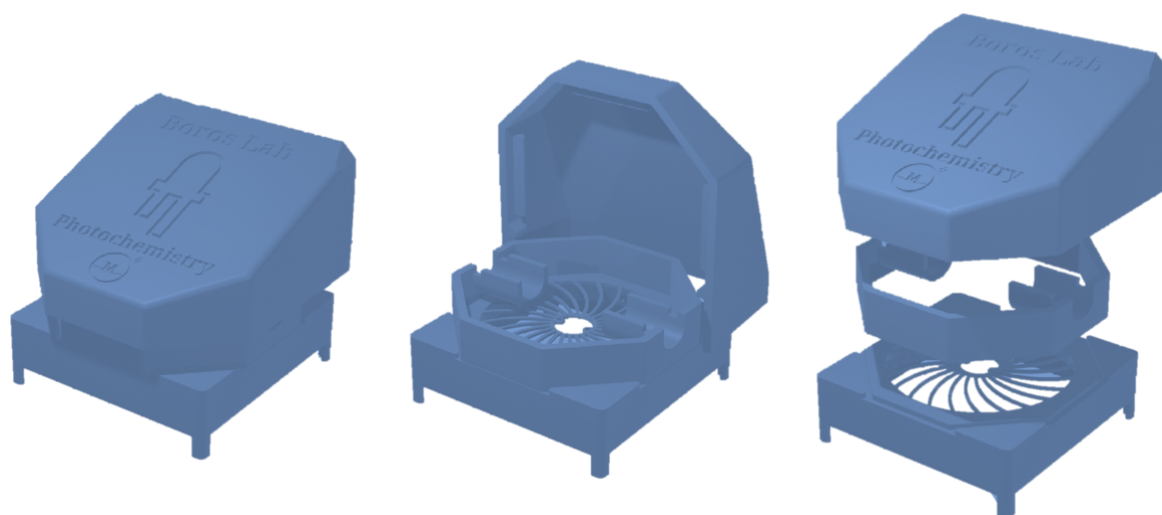


Figure S1. A 3D model of 365 nm photoreactor designed for a 3 mL polypropylene vessel for peptide synthesis with filter.

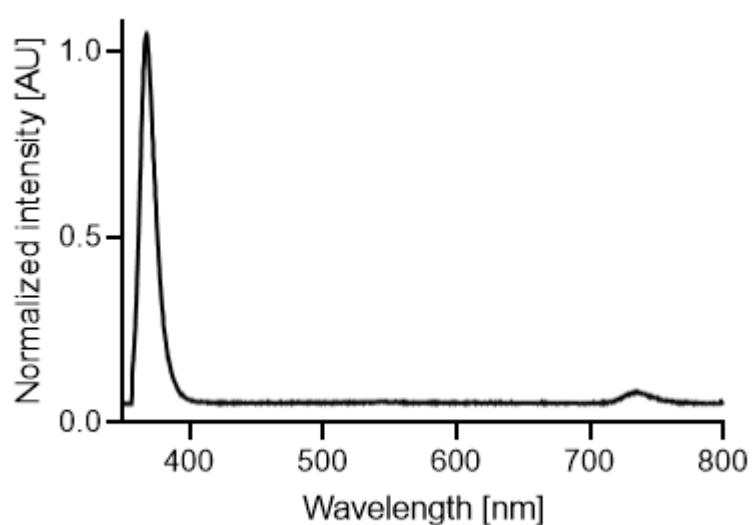


Figure S2. The photon source emission profile (UVA-365 nm-Inolux IN-C68QACTMU2).

2. Synthesis and Characterization of Peptides

2.1 Synthesis of BBN

The synthesis of bombesin (BBN) peptide (**19**) was carried out manually on a 0.05 mmol scale using a tentagel resin (200 mg, 0.26 mmol/g).² The **TG** resin was swollen in DCM (3 mL) and DMF (3 mL) for 1 min three times each. (S)-3-(Fmoc-amino)-3-(2-nitrophenyl)propionic acid (**2**) (68 mg, 0.15 mmol) was coupled to N terminus of the resin using Benzotriazole-1-yl-oxy-tris-pyrrolidino-phosphonium hexafluorophosphate (PyBOP) (54 mg, 0.11 mmol) as coupling reagent in the presence of N,N-Diisopropylethylamine (DIEA) (36 μ L, 0.21 mmol) within 12 h. The Fmoc group was subsequently removed by treatment of the resin with 20% piperidine in DMF (3 mL) for 20 min. Subsequent amino acids were coupled in the same manner until the full sequence (QWAVGHLM) was assembled (see **Scheme S2**). Subsequently, the Fmoc group on N-terminus was deprotected and Fmoc-6-Ahx-OH (74 mg, 0.21 mmol) was coupled using PyBOP (54 mg, 0.11 mmol) as coupling reagent in the presence of DIEA (36 μ L, 0.21 mmol) within 12 h in order to obtain compound **TG-Anp-16**. Finally, the Fmoc group on N-terminus was deprotected and NOTA-bis(t-Bu ester) (65 mg, 0.15 mmol) was coupled using PyBOP (166 mg, 0.32 mmol) as coupling reagent in the presence of DIEA (115 μ L, 0.64 mmol) within 6 h. Eventually, the product **TG-Anp-19** was washed, dried and stored until use.

2.2 Synthesis of PSMA

The synthesis of the PSMA-targeting peptide (**31**, Glu-urea-Lys-nap-trans-Lys-NOTA-ADPA-NH₂) was carried out manually on a 0.16 mmol scale using a Wang resin (200 mg, 0.8 mmol/g) (see **Scheme S3**). The starting material, Glu-urea-Lys-Nap-trans-Lys, was synthesized according our previously established protocol.³ The Lys(Mtt)-trans-nap-Lys-urea-Glu-Wang resin (**WA-20**) (200 mg, 0.16 mmol) was treated with a 1% TFA in DCM to selectively remove the Mtt protecting group. Next, NOTA-bis(t-Bu ester) (199 mg, 0.48 mmol) was coupled to the free amine of the Lys side-chain using PyBOP (166 mg, 0.32 mmol) as a coupling reagent in the presence of DIEA (115 μ L, 0.64 mmol) within 6 h in order to obtain compound **WA-22**. The Fmoc group from N-terminus was removed by shaking the resin with solution of 20% piperidine in DMF for 20 min. The peptide was elongated (**WA-24**) by coupling the adipic acid using PyBOP (166 mg, 0.32 mmol) as the coupling reagent in the presence of DIEA (115 μ L, 0.64 mmol) within 12 h. Subsequently, the NHS active ester of PSMA-targeting peptide (compound **WA-26**) was synthesized by addition of excess of NHS (1104 mg, 8.0 mmol) and EDC (1.522 g, 8.0 mmol) as the coupling reagent in the presence of DIEA (1.39 mL, 8.00 mmol) within 16 h. After coupling, all resin was washed, dried and treated with a mixture of TFA/TIS/H₂O (95%/2.5%/2.5%) to cleave compound **27** from the resin. Compound **27** was purified by reverse-phase semi-preparative HPLC and subsequently re-appended to TG-Anp-H resin. To this end, tentagel resin (200 mg, 0.26 mmol/g) was swollen in DCM and DMF. Next, Fmoc-Anp-OH (67 mg, 0.16 mmol) was coupled to resin using PyBOP (54 mg, 0.10 mmol) as coupling reagent in the presence of DIEA (36 μ L, 0.21 mmol) within 12 h. The Fmoc group was removed by shaking the resin with solution of 20% piperidine in DMF for 25 min. Subsequently, compound **27** (26 mg, 0.02 mmol) was coupled to the

preloaded TG-Anp-H resin in the presence of DIEA ($18 \mu\text{L}$, 0.1 mmol) within 6 h resulting in compound **TG-Anp-31**.

2.3 BBN deprotection

More commonly used deprotection mixtures such as TFA/TIS/ H_2O cause methionine oxidation to sulfoxide in the side chain of the BBN sequence;⁴ accordingly, formation of 15% of BBN peptide with a C-terminal methionine oxide side-product was observed under these conditions. The addition of 1,2-ethanedithiol (EDT) to the cleavage cocktail (cocktail R) reduced the presence of methionine-oxidized analogue to 5% (see **Table S1**). To prevent the formation of oxidized methionine residues in our peptide sequence, the cleavage cocktail containing an $\text{NH}_4\text{I}\text{-Me}_2\text{S}$ (ammonium iodide and dimethylsulfide) was used for acidic deprotection of side chains and terminal cleavage from the resin support. Using the $\text{NH}_4\text{I}\text{-Me}_2\text{S}$ containing cleavage (cocktail H) for the acidic deprotection resulted in only 1% of oxidized side product. To fully eliminate the presence of methionine sulfoxide on the resin support, the amount of $\text{NH}_4\text{I}\text{:Me}_2\text{S}$ reductant pair was increased to 5:10%. Under these conditions, following HPLC analysis, no presence of methionine sulfoxide-peptide was detected (see **Figure S4**). The deprotection has to be carried out each time before radiolabeling, otherwise the oxidation side-product will appear, as shown in **Figure S22**. Any kind of transportation causes the oxidation of BBN.

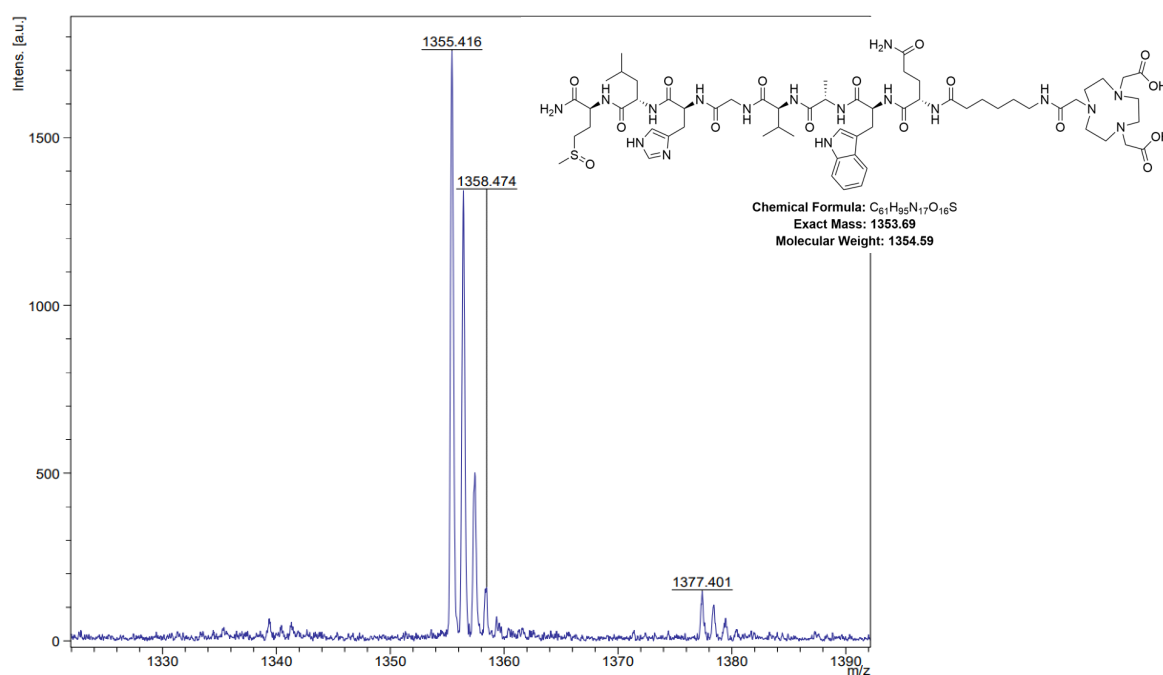


Figure S3. The methionine sulfoxide-containing peptide, side product of NOTA-Aca-BBN (**19**).

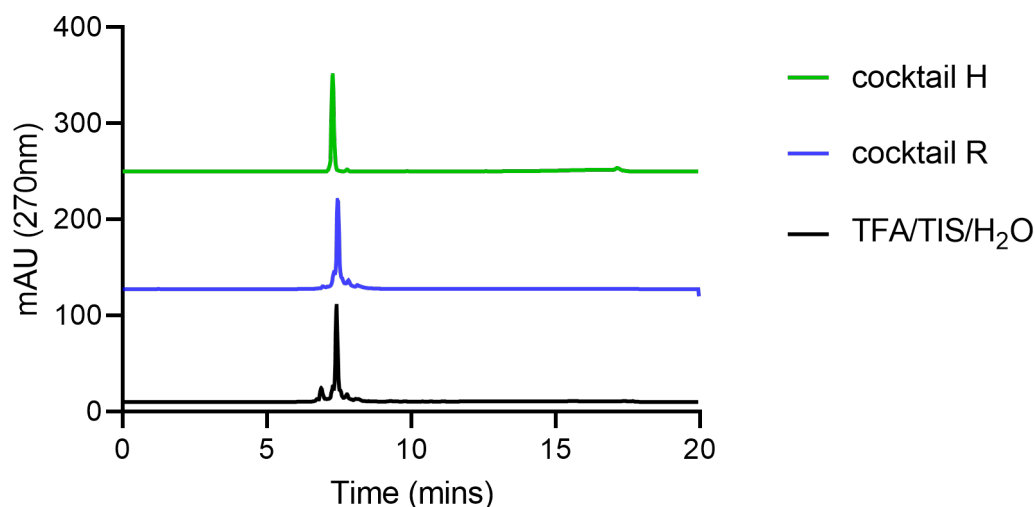


Figure S4. HPLC chromatograms at 270 nm of NOTA-Aca-BBN (**19**) peptide after different deprotection strategies.

2.4 Quantitation of loading efficiency, deprotection and terminal cleavage

Approximation of resin loading. To determine the loading of the resin with respect to peptide conjugation, 5.0 mg of appropriate dry resin was weighed, transferred to a plastic syringe equipped with a filter membrane, and pre-swollen in DCM and DMF. Fmoc deprotection was carried out using standard procedure. All solution was collected through filtration and diluted in ratio 1:25. The UV absorbance was measured at 301 nm in a quartz cuvette with a 1 cm path length to determine the resin loading using the standard formula,⁵

$$\text{Resin loading} = \frac{A(301) \times V \times d}{\epsilon \times W \times m}$$

where $A(301)$ = UV absorbance at 301 nm, V = cleavage volume (2 mL), d = dilution factor (25), ϵ = molar extinction coefficient of Fmoc group ($7800 \text{ mL mmol}^{-1} \text{ cm}^{-1}$), W = cuvette width (1 cm), and m = resin mass in g.

Fmoc deprotection. Fmoc protected peptides were treated with 2 mL of 20% piperidine in DMF (twice, each time 15 min). For the synthesis of all compounds, the N-terminal Fmoc group was deprotected, and after each step the resin was washed with DMF (5 x 2 mL).

TFA cleavage. The resin was suspended in a mixture of TFA/TIS/H₂O (2 mL; 95:2.5:2.5, v/v/v) at room temperature for 3 h. Then, the resin was removed and the residual TFA solution transferred to a 15 mL falcon tube and an ice-cold mixture of Et₂O/hexane (10 mL; 1:1 v/v) was added to precipitate the peptide. The supernatant was removed after centrifugation, and the peptide pellets were washed twice with Et₂O/hexane. The crude peptide precipitate was re-dissolved in MeCN/H₂O (1:1, v/v) and lyophilized, followed by purification by semi-preparative HPLC. Pure fractions were collected and lyophilized characterized by analytical HPLC and MALDI-TOF MS.

Ligand concentration determination (titration). To determine the concentration of ligand solutions like 19 and 31, a spectrophotometric titration was carried out with Cu^{2+} . The formation of $^{\text{nat}}\text{Cu}$ -19 or $^{\text{nat}}\text{Cu}$ -31 was monitored at 270 nm (edge of π - π^*) or 600 nm (d-d) using a 1 cm path length cuvette and a NanoDrop spectrophotometer. The pH was adjusted to 5.5 using 0.25 M ammonium acetate buffer. 110 μM ligand stock solutions were titrated with addition of 90 μM Cu^{2+} aliquots (as determined by ICP-OES) to determine the concentration of ligand by equivalents of Cu^{2+} . The titration endpoint was determined by the inflection point of the change to the absorbance intensity at 270 nm or 280 nm, diagnostic of complex formation, was detected. The HPLC-based calibration curve was measured at 270 nm using 50 μM stock solution of $^{\text{nat}}\text{Cu}$ -19 (determined by ICP-OES) and the slope was determined using simple linear regression in Graph Pad Prism.

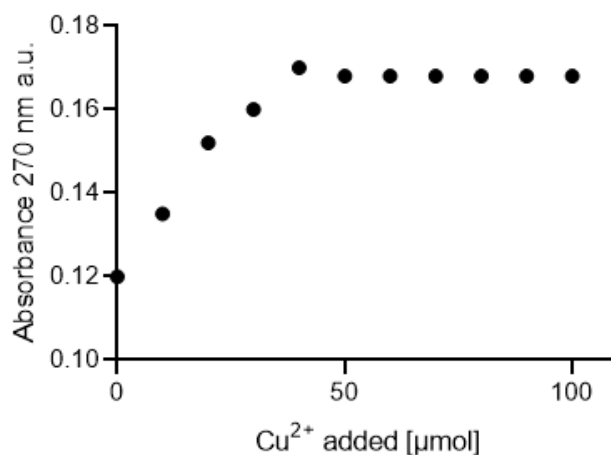


Figure S5. UV-vis titration to endpoint to determine ligand concentrations of 19.

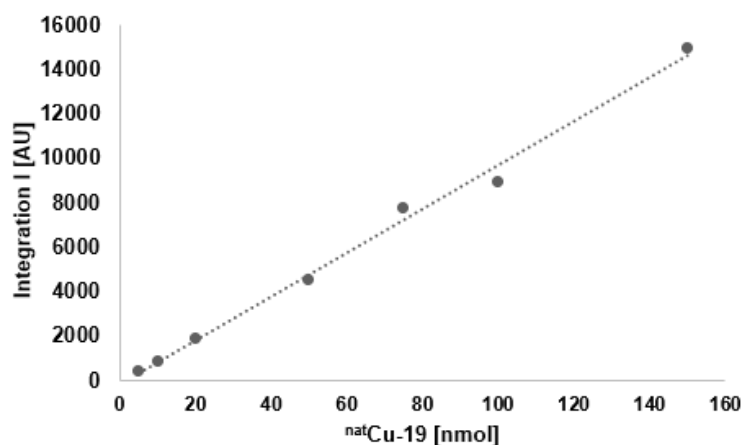


Figure S6. HPLC-based calibration curve measured at 270 nm using 50 μM stock solution of $^{\text{nat}}\text{Ga}$ -19 (determined by ICP-OES).

Table S1. Reagents and conditions for NOTA-Aca-BBN (**19**) deprotection.

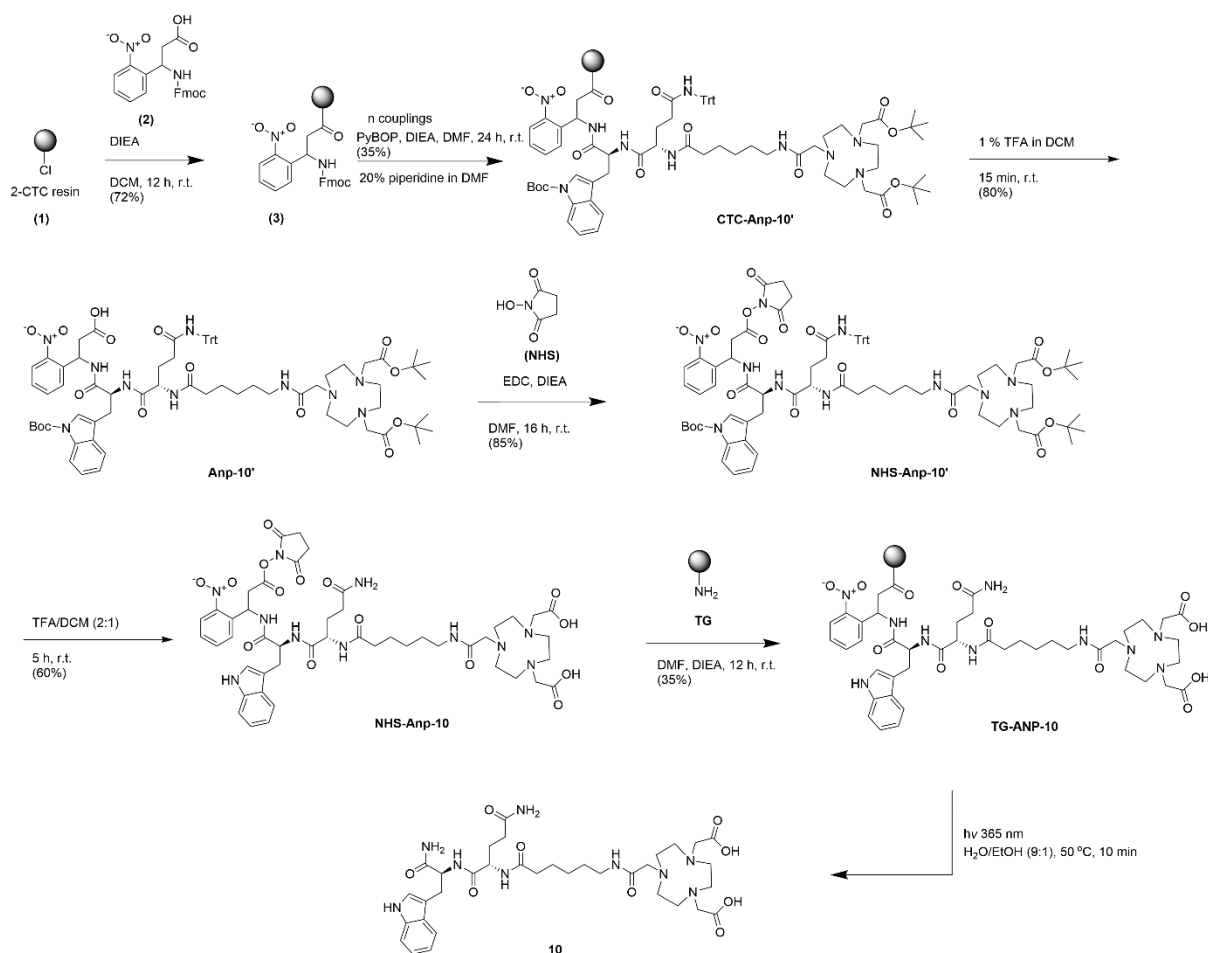
Entry	Deprotection mixture	Time [h]	Side-product [%]	NOTA-Aca-BBN (19) [%]
1	TFA/TIS/H ₂ O (95%/2.5%/2.5%) (standard cocktail)	1	15	85
2	TFA/TIS/H ₂ O (95%/2.5%/2.5%) (standard cocktail)	3	15	85
3	TFA/TIS/EDT/H ₂ O (90%/2.5%/5.0%/2.5%) (cocktail R)	1	15	85
4	TFA/TIS/EDT/H ₂ O (90%/2.5%/5.0%/2.5%)	3	15	85

	(cocktail R)			
5	TFA/TIS/TA/(CH ₃) ₂ S/NH ₄ I/H ₂ O (80%/5.0%/5.0%/5.0%/2.5%/2.5%) (cocktail H)	1	5	95
6	TFA/TIS/TA/(CH ₃) ₂ S/NH ₄ I/H ₂ O (80%/5.0%/5.0%/5.0%/2.5%/2.5%) (cocktail H)	3	5	95
7	TFA/Phenol/TA/EDT/(CH ₃) ₂ S/NH ₄ I/H ₂ O (80%/2.5%/5.0%/2.5%/5.0%/2.5%/2.5%) (cocktail H)	1	1	99
8	TFA/Phenol/TA/EDT/(CH ₃) ₂ S/NH ₄ I/H ₂ O (80%/2.5%/5.0%/2.5%/5.0%/2.5%/2.5%) (cocktail H)	3	1	99
9	TFA/Phenol/TA/EDT/(CH₃)₂S/NH₄I/H₂O (70%/5.0%/5.0%/2.5%/10%/5.0%/2.5%) (cocktail H)	1	-	100
10	TFA/Phenol/TA/EDT/(CH₃)₂S/NH₄I/H₂O (70%/5.0%/5.0%/2.5%/10%/5.0%/2.5%) (cocktail H)	3	-	100

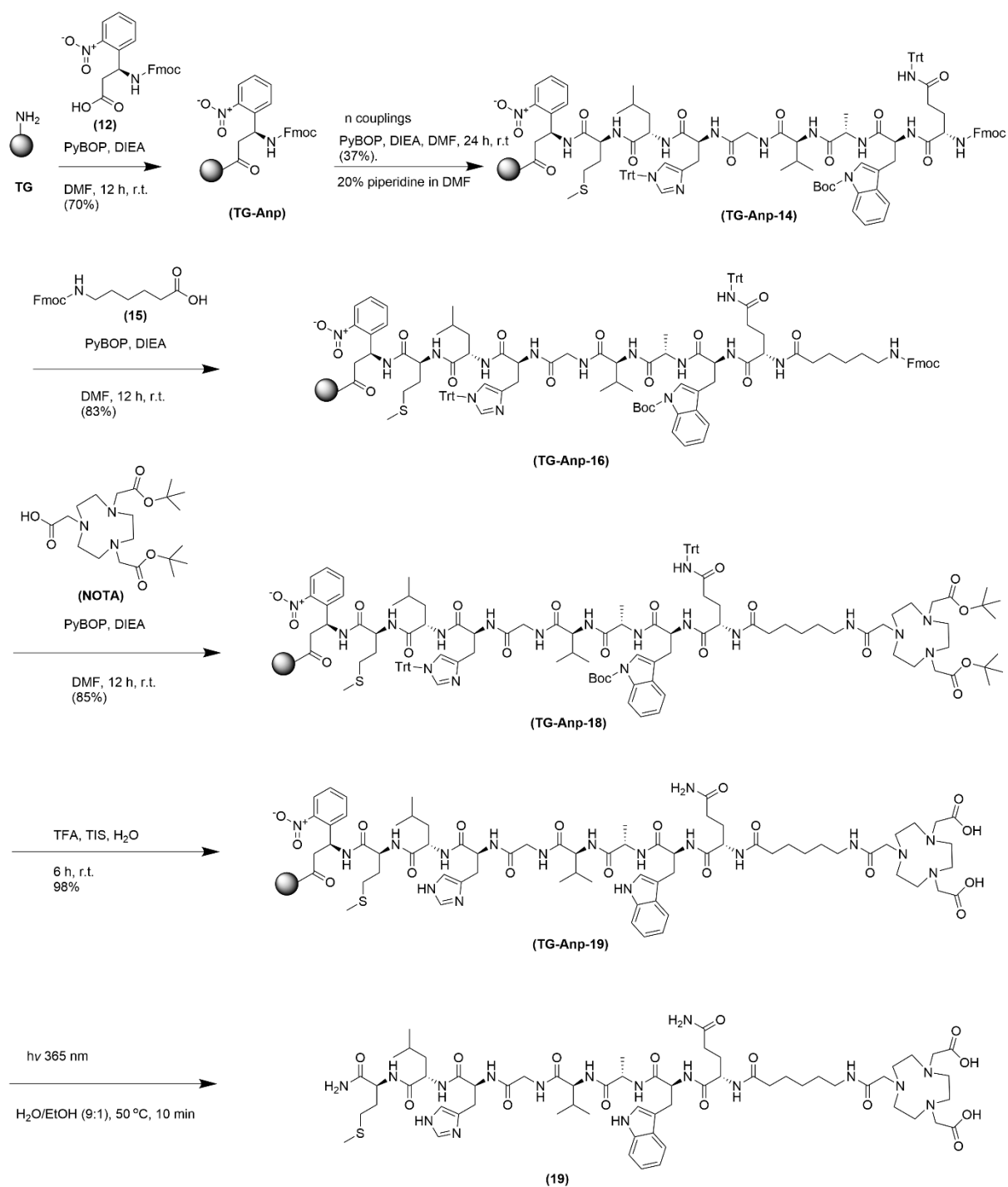
2.5 Photocleavage

The appropriate Anp-linked resin was suspended in 10% ethanol in H₂O in a filter frit endowed plastic syringe. The syringe was subsequently placed inside the photoreactor and reacted under gentle agitation and cooling with the built-in fan and photoirradiation with the 365 nm LED light source. After photocleavage, the product was filtered and characterized by HPLC (or radio-HPLC) HR-ESI-MS or MALDI-TOF MS.

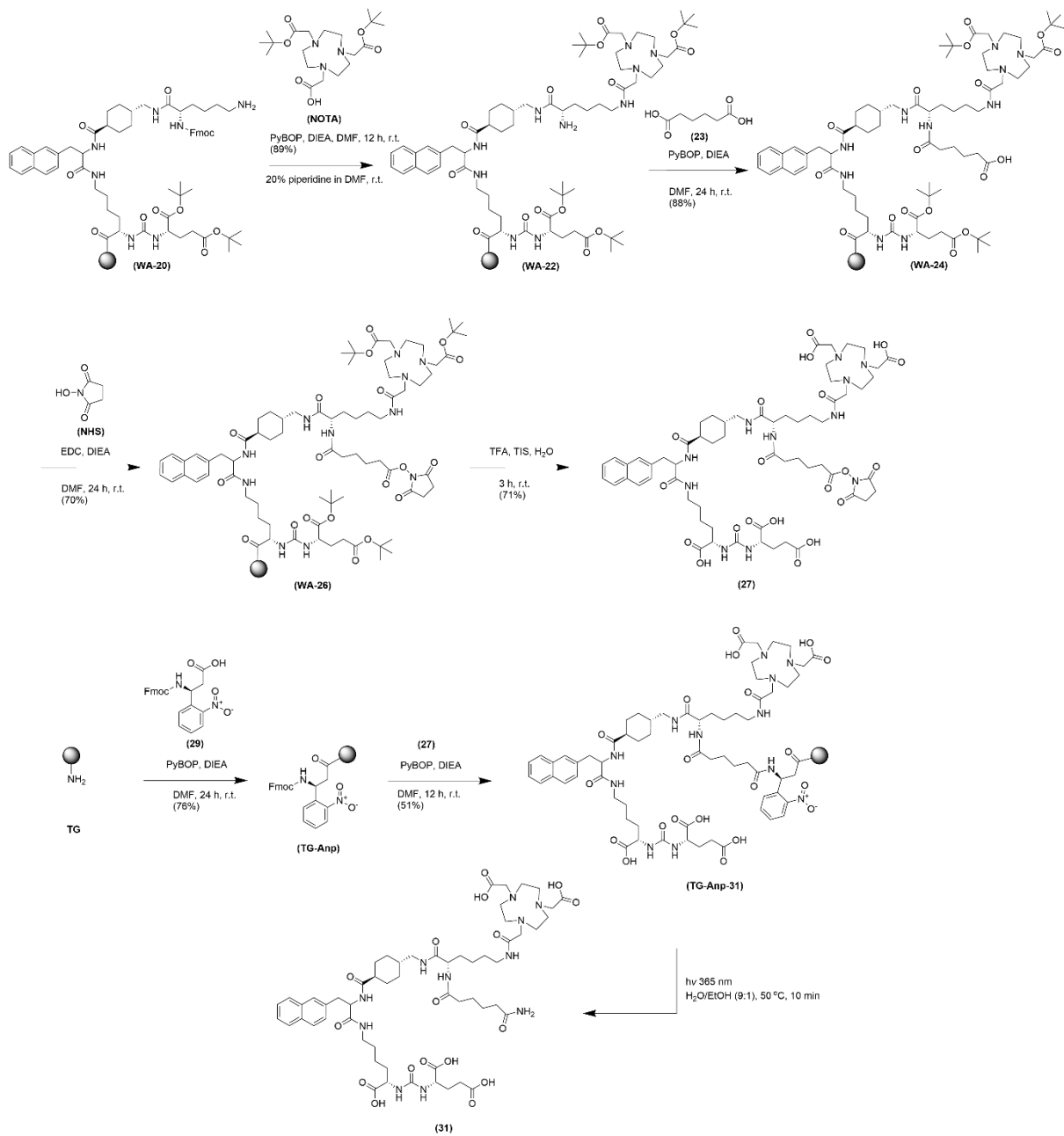
2.6 Synthesis of ligands



Scheme S1. Synthesis pathway of TG-Anp-10 and 10.



Scheme S2. Synthesis pathway of **TG-Anp-19** and **19**.



Scheme S3. Synthesis of TG-Anp-31 and 31.

2.7 HRMS, MALDI and HPLC characterization data

(11*S*,14*S*)-1-(4,7-bis(2-(*tert*-butoxy)-2-oxoethyl)-1,4,7-triazonan-1-yl)-14-((1-(*tert*-butoxycarbonyl)-1*H*-indol-3-yl)methyl)-17-(2-nitrophenyl)-2,9,12,15-tetraoxo-11-(3-oxo-3-(tritylamino)propyl)-3,10,13,16-tetraazanonadecan-19-oic acid, (**Anp-10'**). The intermediate **Anp-10'** (50 mg, 0.12 mmol) was synthesized from compound **1** using standard SPPS strategy outlined in **Scheme S1**. The product was isolated as a colorless solid following deprotection and characterized using mass spectrometry and HPLC chromatography. Yield: (0.023 g, 80 %). R_t (Method A): 13.4 min. HR-ESI-MS $[M+H]^+$ calc. for $C_{75}H_{96}N_{10}O_{15}$ 1377.7134, found 1377.7129.

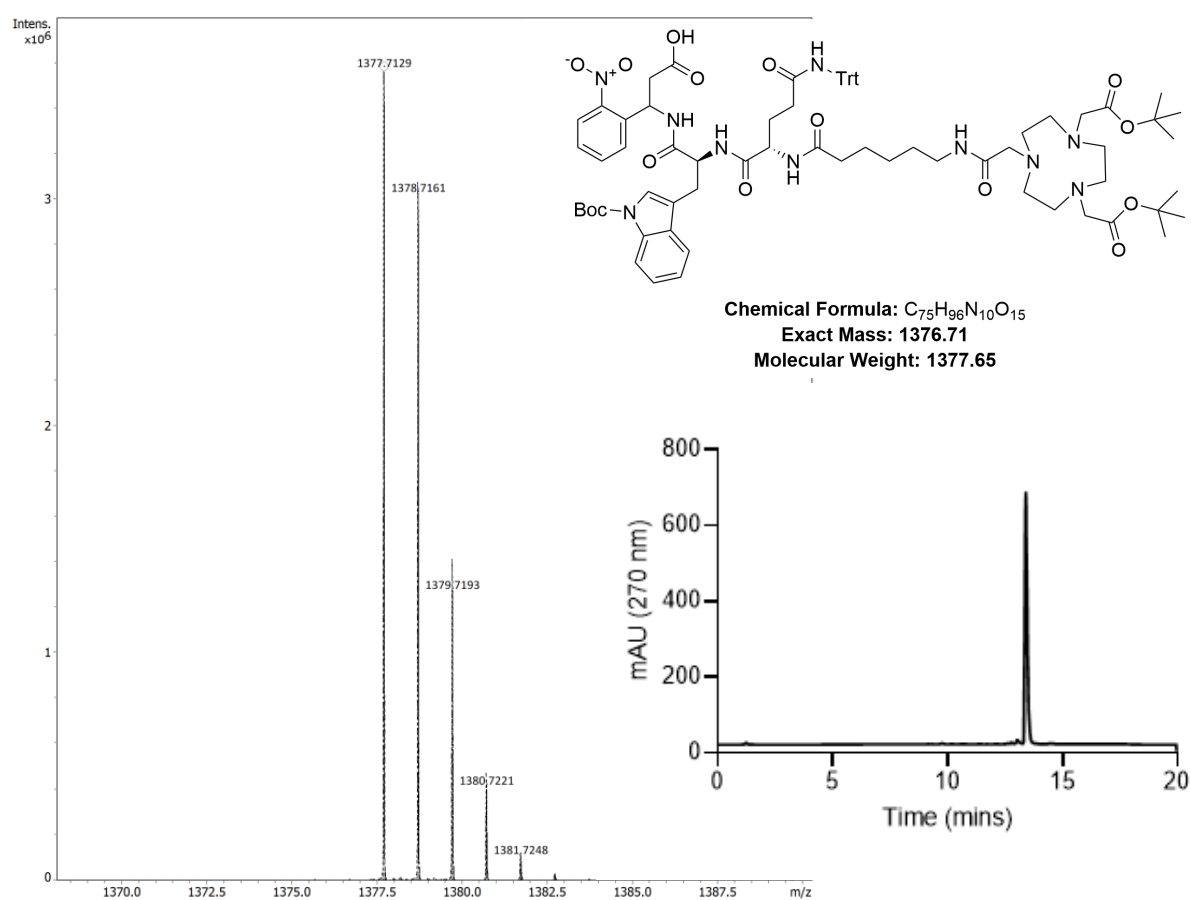


Figure S7. Characterization data for intermediate **Anp-10'**.

*Di-tert-butyl 2,2'-(7-((1*S*,14*S*)-14-((1-(*tert*-butoxycarbonyl)-1*H*-indol-3-yl)methyl)-19-((2,5-dioxopyrrolidin-1-yl)oxy)-17-(2-nitrophenyl)-2,9,12,15,19-pentaoxo-11-(3-oxo-3-(tritylamino)propyl)-3,10,13,16-tetraazanadecyl)-1,4,7-triazonane-1,4-diyl)diacetate, (NHS-Anp-10')*. Intermediate **NHS-Anp-10'** (50 mg, 0.12 mmol) was synthesized using NHS/EDC coupling strategy from compound **Anp-10'** outlined in **Scheme S1**. The product was isolated as a colorless solid following deprotection and characterized using mass spectrometry and HPLC chromatography. Yield: (0.025 g, 85 %). R_t (Method A): 13.7 min. HR-ESI-MS $[M+H]^+$ calc. for $C_{79}H_{99}N_{11}O_{17}$ 1474.7298, found 1474.7290.

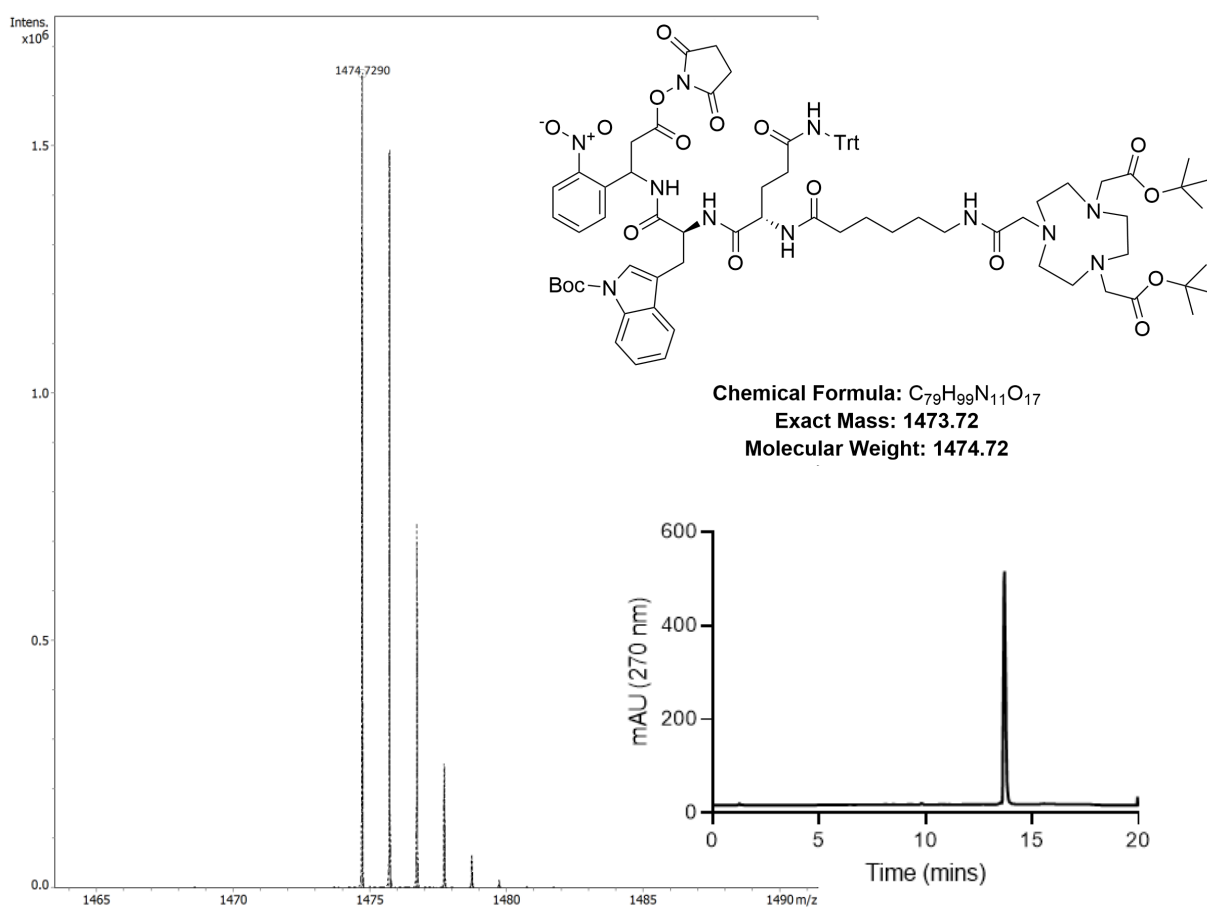


Figure S8. Characterization data for intermediate **NHS-Anp-10'**.

2,2'-(7-((1*S*,14*S*)-14-((1*H*-indol-3-yl)methyl)-11-(3-amino-3-oxopropyl)-19-((2,5-dioxopyrrolidin-1-yl)oxy)-17-(2-nitrophenyl)-2,9,12,15,19-pentaoxo-3,10,13,16-tetraazonadecyl)-1,4,7-triazonane-1,4-diyl)diacetic acid, (**NHS-Anp-10**). Intermediate **NHS-Anp-10** (50 mg, 0.12 mmol) was synthesized using standard deprotection strategy outlined in **Section 2.4** from compound **NHS-Anp-10'**. The product was isolated as a colorless solid following deprotection and characterized using mass spectrometry and HPLC chromatography. Yield: (0.011 g, 60 %). R_t (Method A): 8.27 min. HR-ESI-MS $[M+H]^+$ calc. for $C_{47}H_{61}N_{11}O_{15}$ 1020.4426, found 1020.4413.

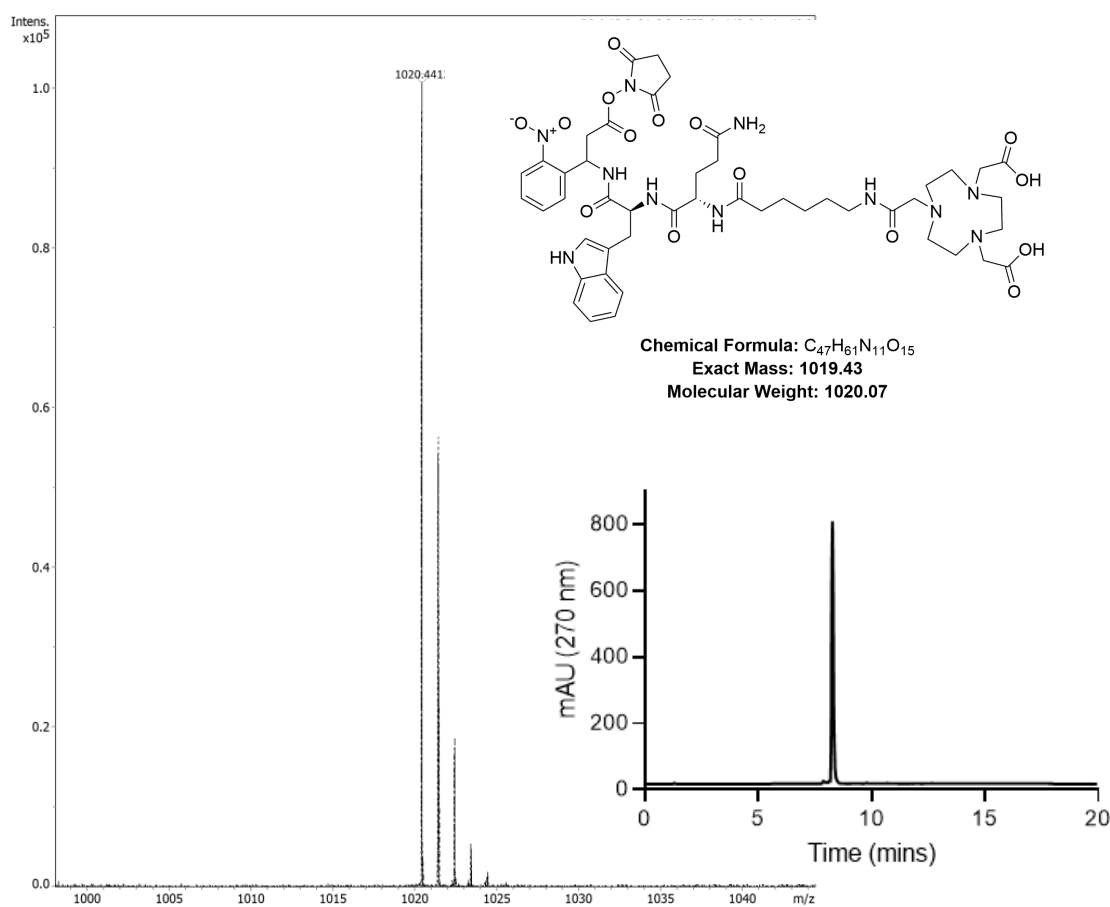


Figure S9. Characterization data for intermediate **NHS-Anp-10**.

2,2'-(7-(2-((6-(((S)-5-amino-1-(((S)-1-amino-3-(1H-indol-3-yl)-1-oxopropan-2-yl)amino)-1,5-dioxopentan-2-yl)amino)-6-oxohexyl)amino)-2-oxoethyl)-1,4,7-triazonane-1,4-diyl)diacetic acid, (**10**). Compound **10** (50 mg, 0.12 mmol) was synthesized by photocleavage outlined in **Section 2.5** and **Scheme S1** from compound **TG-Anp-10**. The product was isolated as a colorless solid following deprotection and characterized using mass spectrometry and HPLC chromatography. Yield: (0.009 g, 40 %). R_t (Method A): 6.47 min. HR-ESI-MS $[M+H]^+$ calc. for $C_{34}H_{51}N_9O_9$ 730.3888, found 730.3881.

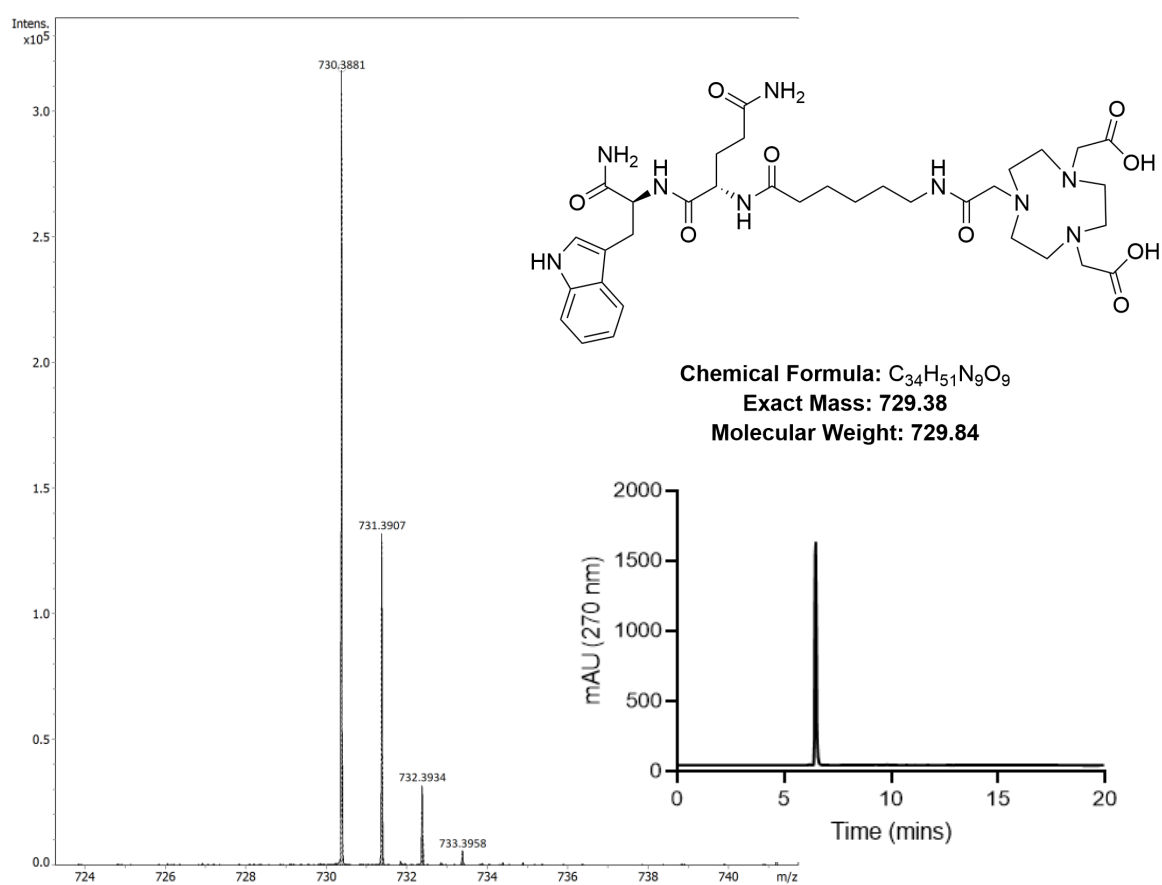


Figure S10. Characterization data for intermediate **10**.

(*S*)-*N*1-((5*S*,8*S*,11*S*,17*S*,20*S*,23*S*)-11-((1*H*-imidazol-4-yl)methyl)-5-carbamoyl-24-(1*H*-indol-3-yl)-8-isobutyl-17-isopropyl-20-methyl-7,10,13,16,19,22-hexaoxo-2-thia-6,9,12,15,18,21-hexaazatetracosan-23-yl)-2-aminopentanediamide, (**14**). Intermediate **14** (50 mg, 0.12 mmol) was synthesized using the general coupling strategy outlined in **Section 2.1** and **Scheme S2** from deprotected compound **TG-Anp-14**. The product was isolated as a colorless solid following deprotection and characterized using mass spectrometry and HPLC chromatography. Yield: (0.010 g, 37 %). R_t (Method A): 7.30 min. MALDI $[M+H]^+$ calc. for $C_{43}H_{65}N_{13}O_9S$ 940.4827, found 941.040.

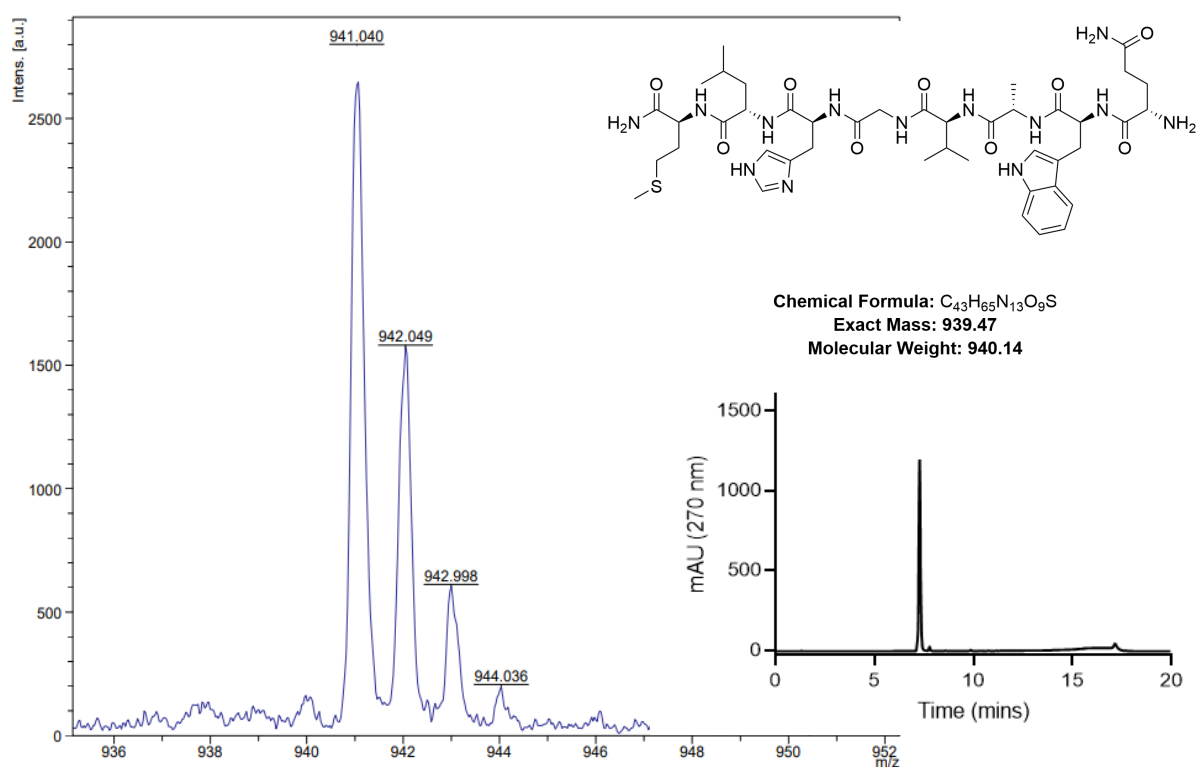


Figure S11. Characterization data for intermediate **14**.

(*S*)-*N*1-((*5S,8S,11S,17S,20S,23S*)-11-((*1H*-imidazol-4-yl)methyl)-5-carbamoyl-24-(*1H*-indol-3-yl)-8-isobutyl-17-isopropyl-20-methyl-7,10,13,16,19,22-hexaoxo-2-thia-6,9,12,15,18,21-hexaazatetracosan-23-yl)-2-(6-aminohexanamido)pentanediamide, (**16**). Intermediate **16** (50 mg, 0.12 mmol) was synthesized using the general coupling strategy outlined in **Section 2.1** and **Scheme S2** from deprotected compound **TG-Anp-16**. The product was isolated as a colorless solid following deprotection and characterized using mass spectrometry and HPLC chromatography. Yield: (0.025 g, 83 %). R_t (Method A): 7.25 min. MALDI-MS $[M+H]^+$ calc. for $C_{49}H_{76}N_{14}O_{10}S$ 1053.5667, found 1054.256.

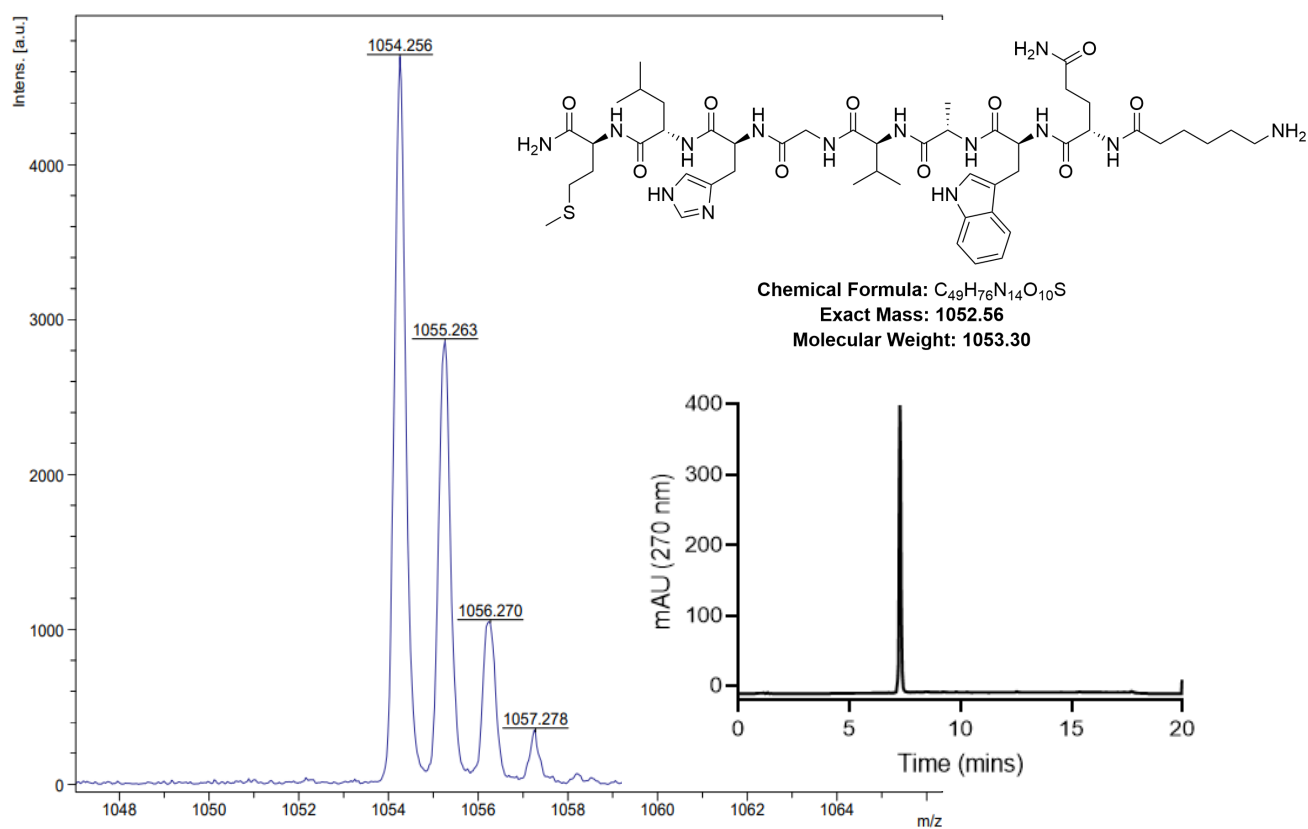


Figure S12. Characterization data for intermediate **16**.

2,2'-(7-((5*S*,8*S*,11*S*,17*S*,20*S*,23*S*,26*S*)-11-((1*H*-imidazol-4-yl)methyl)-23-((1*H*-indol-3-yl)methyl)-26-(3-amino-3-oxopropyl)-5-carbamoyl-8-isobutyl-17-isopropyl-20-methyl-7,10,13,16,19,22,25,28,35-nonaoxo-2-thia-6,9,12,15,18,21,24,27,34-nonaazahexatriacontan-36-yl)-1,4,7-triazonane-1,4-diyl)diacetic acid, (**19**). Compound **19** (50 mg, 0.12 mmol) was synthesized using the general coupling strategy outlined in **Section 2.1** and **Scheme S2** from compound **TG-Anp-19**. The product was isolated as a colorless solid following deprotection and characterized using mass spectrometry and HPLC chromatography. Yield: (0.010 g, 41 %). R_t (Method A): 7.42 min. MALDI-MS $[M+H]^+$ calc. for $C_{61}H_{95}N_{17}O_{15}S$ 1338.6992, found 1339.477.

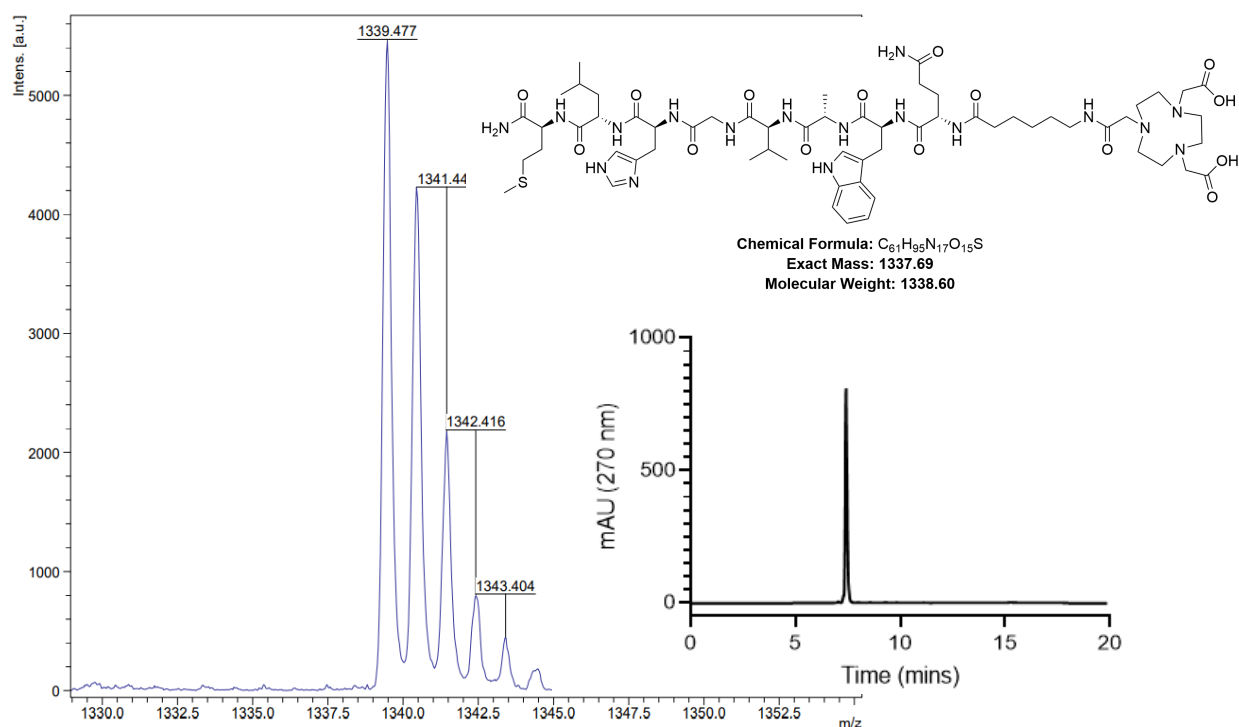


Figure S13. Characterization data for intermediate **19**.

((*(1S)*-5-(2-((*(1S,4S)*-4-(((*(S)*-2-amino-6-(2-(4,7-bis(carboxymethyl)-1,4,7-triazonan-1-yl)acetamido)hexanamido)methyl)cyclohexane-1-carboxamido)-3-(naphthalen-2-yl)propanamido)-1-carboxypentyl)carbamoyl)-*L*-glutamic acid, (**22**). Intermediate **22** (50 mg, 0.12 mmol) was synthesized using the general coupling strategy outlined in **Section 2.2** and **Scheme S3** from deprotected compound **WA-22**. The product was isolated as a colorless solid following deprotection and characterized using mass spectrometry and HPLC chromatography. Yield: (0.029 g, 89 %). R_t (Method A): 7.35 min. HR-ESI-MS $[M+H]^+$ calc. for $C_{51}H_{76}N_{10}O_{15}$ 1069.5569, found 1069.5576.

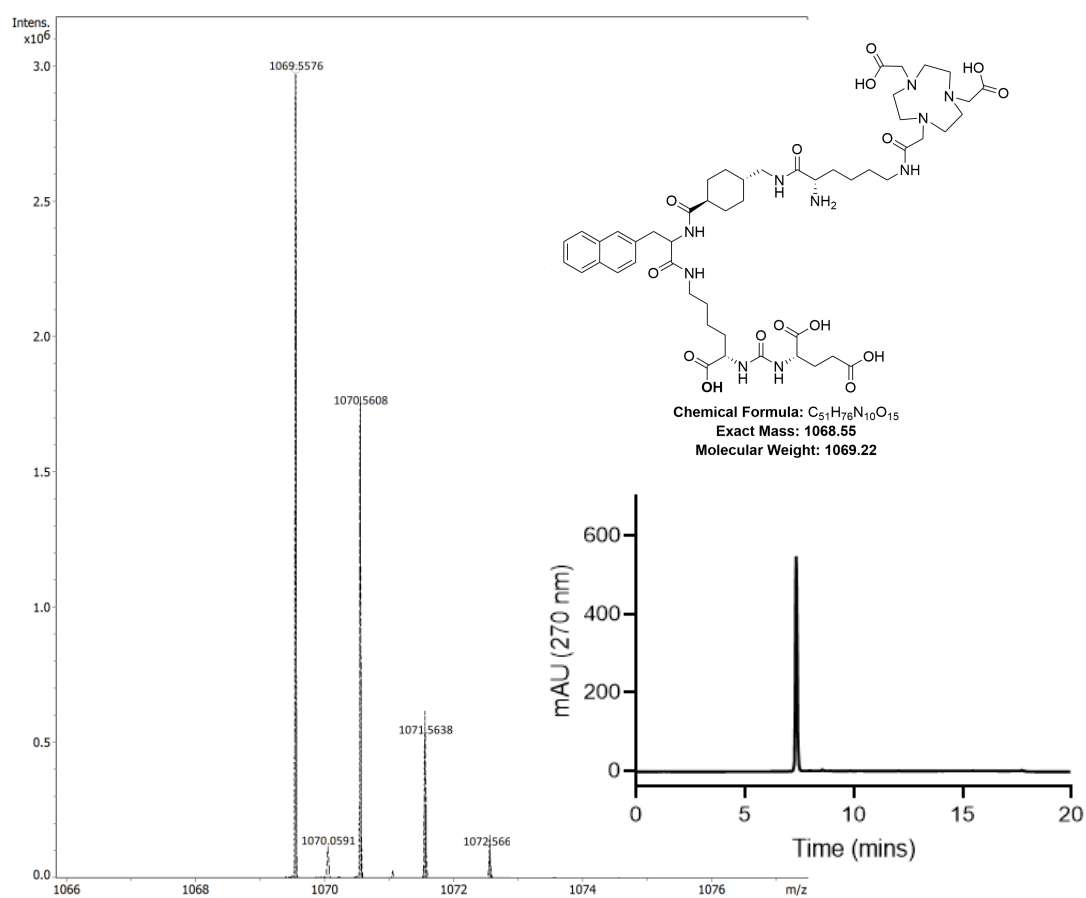


Figure S14. Characterization data for intermediate **22**.

(((1*S*)-5-(2-((1*S*,4*S*)-4-(((*S*)-6-(2-(4,7-bis(carboxymethyl)-1,4,7-triazonan-1-yl)acetamido)-2-(5-carboxypentanamido)hexanamido)methyl)cyclohexane-1-carboxamido)-3-(naphthalen-2-yl)propanamido)-1-carboxypentyl)carbamoyl)-*L*-glutamic acid, (**24**). Intermediate **24** (50 mg, 0.12 mmol) was synthesized using the general coupling strategy outlined in **Section 2.2** and **Scheme S3** from deprotected compound **WA-24**. The product was isolated as a colorless solid following deprotection and characterized using mass spectrometry and HPLC chromatography. Yield: (0.028 g, 88 %). R_t (Method A): 7.48 min. HR-ESI-MS $[M+H]^+$ calc. for $C_{57}H_{84}N_{10}O_{18}$ 1197.6043, found 1197.6024.

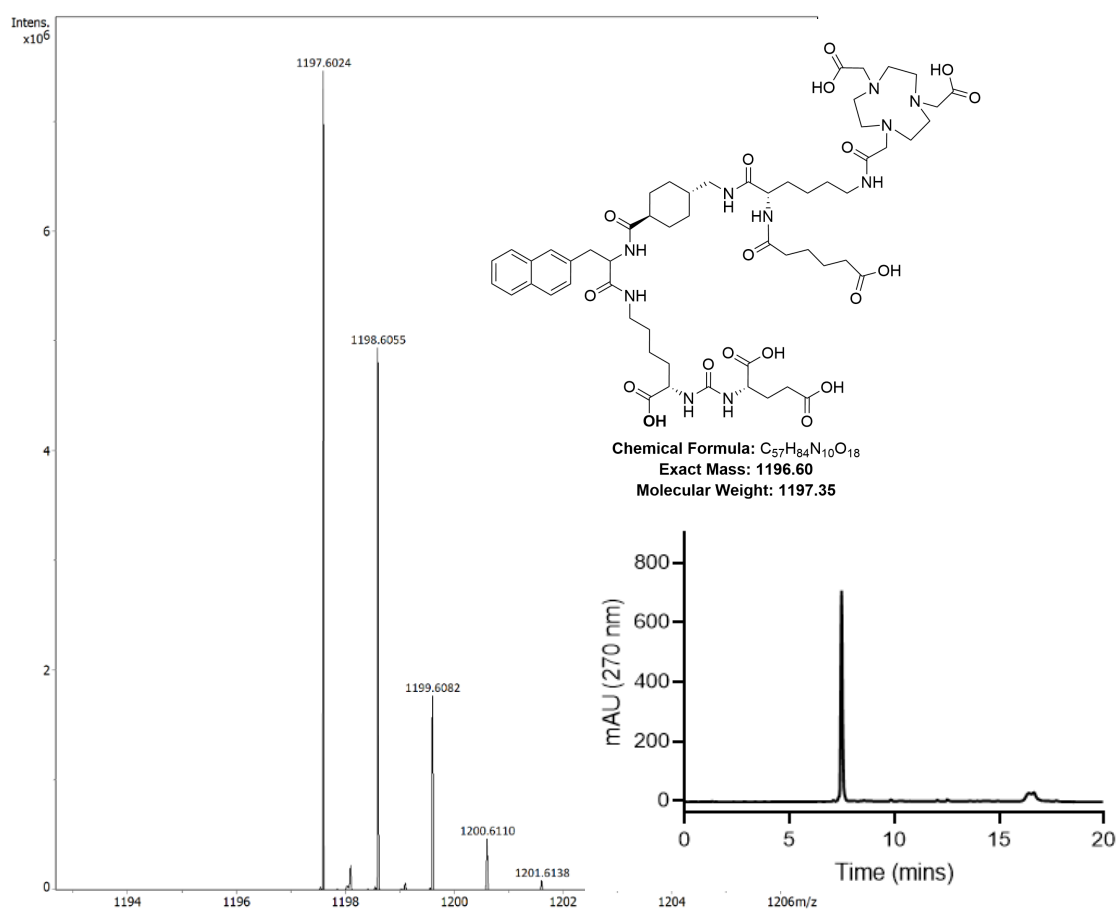


Figure S15. Characterization data for intermediate **24**.

((*1S*)-5-(2-((*1S,4S*)-4-(((*S*)-6-(2-(4,7-bis(carboxymethyl)-1,4,7-triazonan-1-yl)acetamido)-2-(6-((2,5-dioxopyrrolidin-1-yl)oxy)-6-oxohexanamido)hexanamido)methyl)cyclohexane-1-carboxamido)-3-(naphthalen-2-yl)propanamido)-1-carboxypentyl)carbamoyl)-*L*-glutamic acid, (**27**). The intermediate **27** (50 mg, 0.12 mmol) was synthesized using the NHS/EDC coupling strategy outlined in **Section 2.2** and **Scheme S3** from compound **WA-26**. The product was isolated as a colorless solid following deprotection and characterized using mass spectrometry and HPLC chromatography. Yield: (0.022 g, 70 %). R_t (Method A): 8.27 min. MALDI-MS $[M+H]^+$ calc. for $C_{61}H_{87}N_{11}O_{20}$ 1294.6207, found 1294.547.

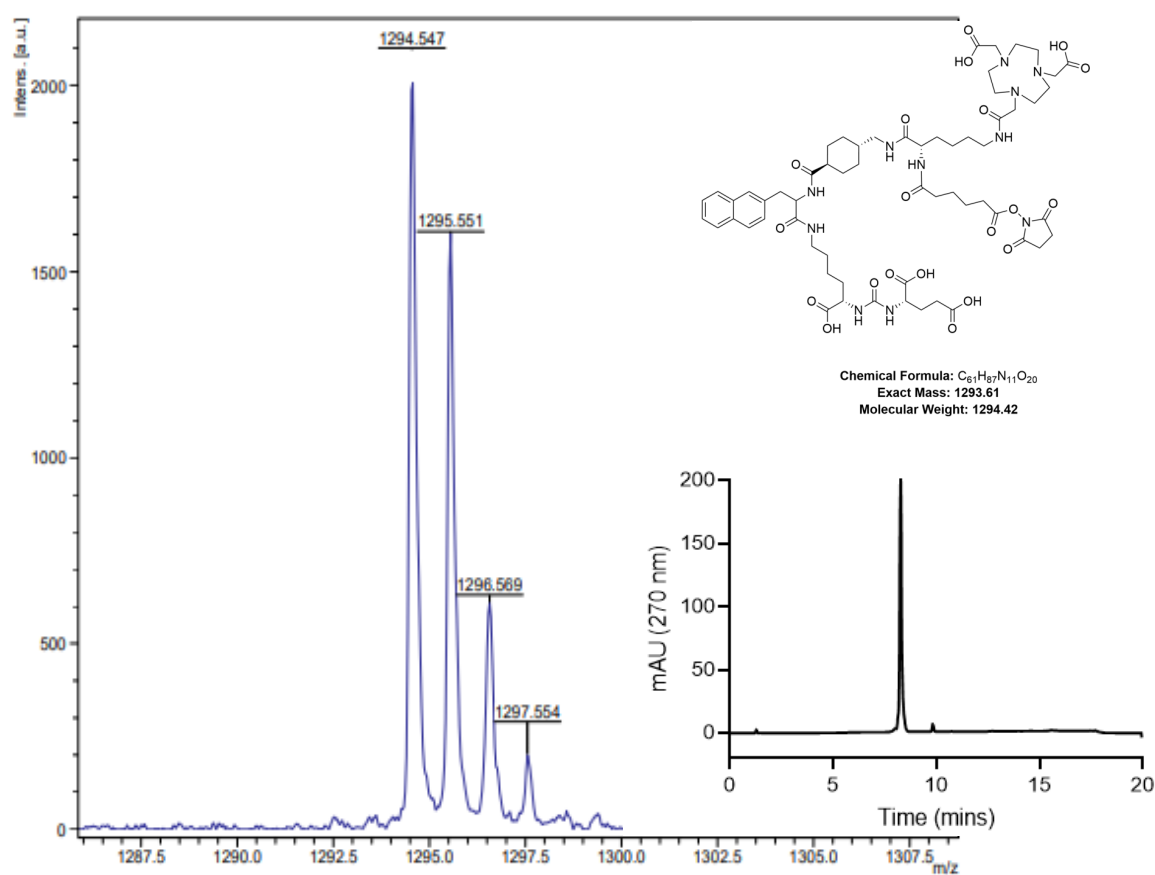


Figure S16. Characterization data for intermediate **27**.

((*(1S)*-5-(2-((*(1S,4S)*-4-(((*(S)*-2-(6-amino-6-oxohexanamido)-6-(2-(4,7-bis(carboxymethyl)-1,4,7-triazonan-1-yl)acetamido)hexanamido)methyl)cyclohexane-1-carboxamido)-3-(naphthalen-2-yl)propanamido)-1-carboxypentyl)carbamoyl)-*L*-glutamic acid, (**31**). Compound **31** (50 mg, 0.12 mmol) was synthesized using the general coupling strategy outlined in **Section 2.2** and **Scheme S3** followed by photocleavage (**Section 2.5**) from compound **TG-Anp-31**. The product was isolated as a colorless solid following deprotection and characterized using mass spectrometry and HPLC chromatography. Yield: (0.007 g, 33 %). R_t (Method A): 7.42 min. MALDI-MS $[M+H]^+$ calc. for $C_{57}H_{85}N_{11}O_{17}$ 1196.6203, found 1195.769.

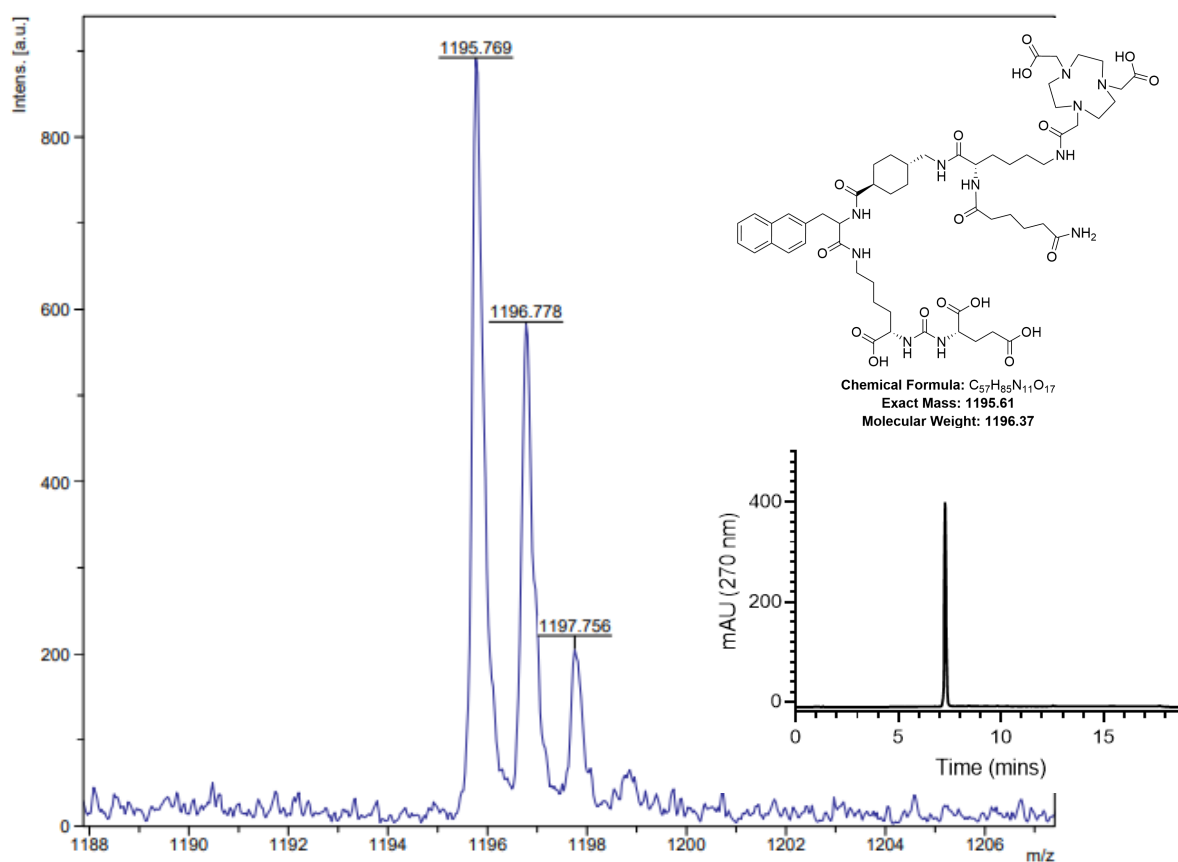
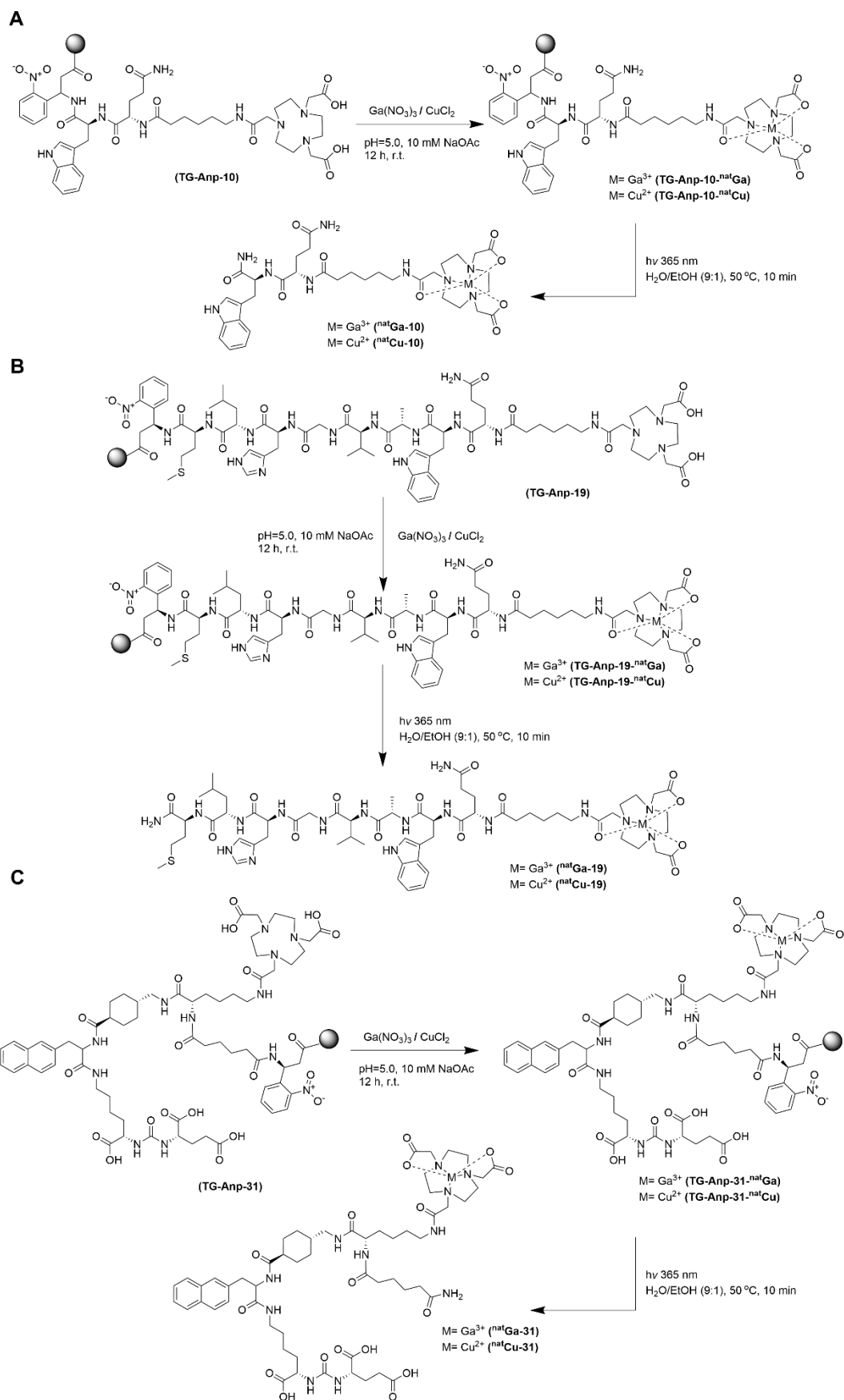


Figure S17. Characterization data for **31**.

3. Synthesis and Characterization of Coordination Complexes

3.1 General Complexation Protocol

The resin-appended peptide, **Anp-10** (2.0 mg, 100 nmol), **Anp-19** (1.0 mg, 100 nmol) or **Anp-31** (4.0 mg, 100 nmol), was washed with 3 mL of DCM, DMF, H₂O and 10 mM NaOAc buffer (pH=5.0) three times each for 1 min. Next, the aqueous stock solutions of Ga³⁺ or Cu²⁺ were prepared and an aliquot of the resin corresponding to one equivalent was added and the complexation was carried out at room temperature for 12 h in pH 5 NaOAc buffer. The metal-peptide conjugates were subsequently photocleaved and the formation of complexed molecule was affirmed with analytical HPLC and mass spectrometry (ESI-MS and MALDI-TOF). The complex conjugates were then purified via semi-preparative HPLC.



Scheme S4. Synthesis of isotopically stable complexes.

3.2 HRMS, MALDI and HPLC data of Coordination complexes

Gallium 2,2'-(7-((5*S*,8*S*)-5-((1*H*-indol-3-yl)methyl)-8-(3-amino-3-oxopropyl)-1-carboxy-2-(2-nitrophenyl)-4,7,10,17-tetraoxo-3,6,9,16-tetrazaoctadecan-18-yl)-1,4,7-triazonane-1,4-diyl)diacetate (^{nat}Ga-Anp-10), Compound ^{nat}Ga-Anp-10 was synthesized using the generalized complexation procedure (Section 3.1) from deprotected compound Anp-10. The product was isolated as a pale yellow solid following deprotection and characterized using mass spectrometry and HPLC chromatography. Yield: (32 nmol, 32 %). R_t (Method A): 7.62 min. MALDI-MS [M]⁺ calc. for C₄₃H₅₆GaN₁₀O₁₃ 989.3384, found 989.445.

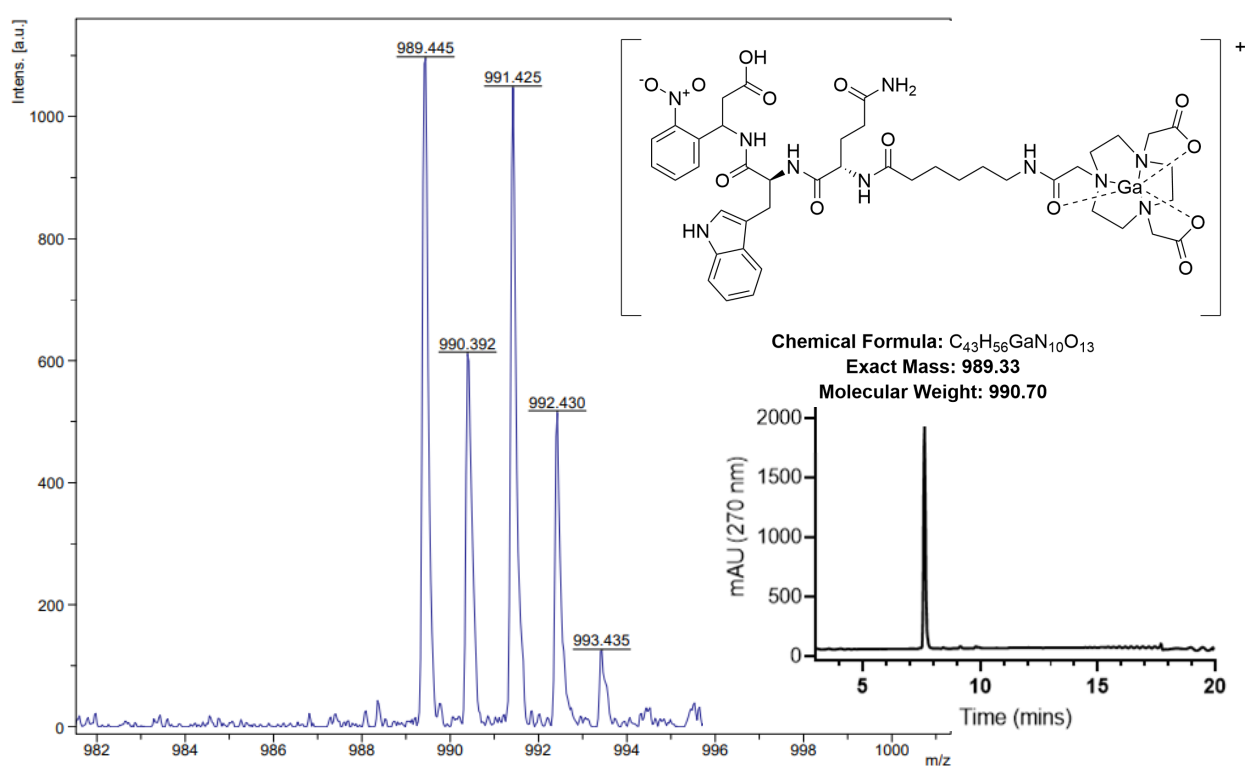


Figure S18. Characterization data for complex ^{nat}Ga-Anp-10.

Copper 2,2'-(7-((5*S*,8*S*)-5-((1*H*-indol-3-yl)methyl)-8-(3-amino-3-oxopropyl)-1-carboxy-2-(2-nitrophenyl)-4,7,10,17-tetraoxo-3,6,9,16-tetraazaocadecan-18-yl)-1,4,7-triazonane-1,4-diyl)diacetate, (^{nat}Cu-10), Compound ^{nat}Cu-10 was synthesized using the generalized complexation procedure (Section 3.1) outlined in Scheme S4A followed by photocleavage (Section 2.5) from compound TG-Anp-10-^{nat}Cu. The product was isolated as a pale blue solid following deprotection and characterized using mass spectrometry and HPLC chromatography. Yield: (30 nmol, 30 %). R_t (Method A): 6.12 min. MALDI-MS [M+H]⁺ calc. for C₃₄H₄₉CuN₉O₉ 791.3027, found 791.333.

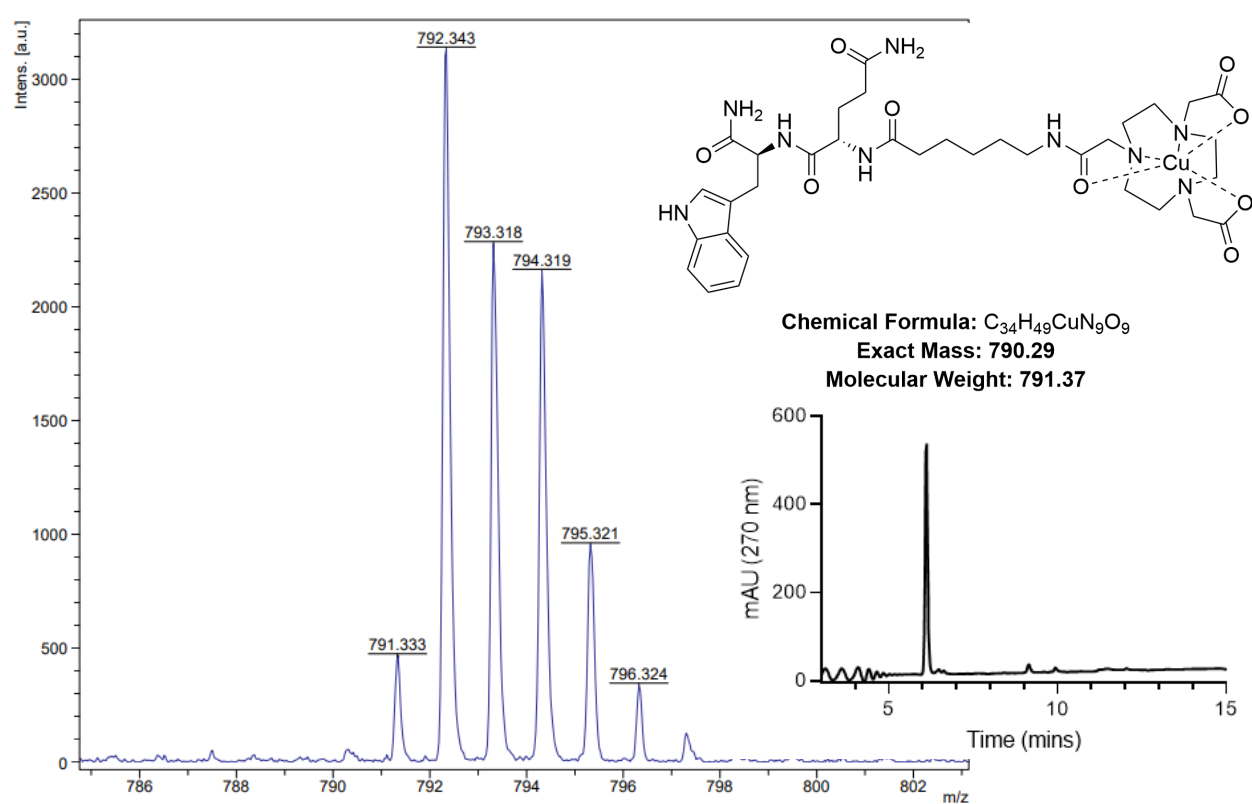


Figure S19. Characterization data for complex ^{nat}Cu-10.

Gallium 2,2'-(7-((5S,8S,11S,17S,20S,23S,26S)-11-((1H-imidazol-4-yl)methyl)-23-((1H-indol-3-yl)methyl)-26-(3-amino-3-oxopropyl)-5-carbamoyl-8-isobutyl-17-isopropyl-20-methyl-7,10,13,16,19,22,25,28,35-nonaaxo-2-thia-6,9,12,15,18,21,24,27,34-nonaazahexatriacontan-36-yl)-1,4,7-triazonane-1,4-diyl)diacetic acetate, (^{nat}Ga-19), Compound ^{nat}Ga-19 was synthesized using the generalized complexation procedure (Section 3.1) outlined in Scheme S4B followed by photocleavage (Section 2.5) from compound TG-Anp-19-^{nat}Ga. The product was isolated as a pale yellow solid following deprotection and characterized using mass spectrometry and HPLC chromatography. Yield: (35 nmol, 35 %). R_t (Method A): 7.25 min. MALDI [M]⁺ calc. for C₆₁H₉₃GaN₁₇O₁₅S 1404.6014, found 1405.544.

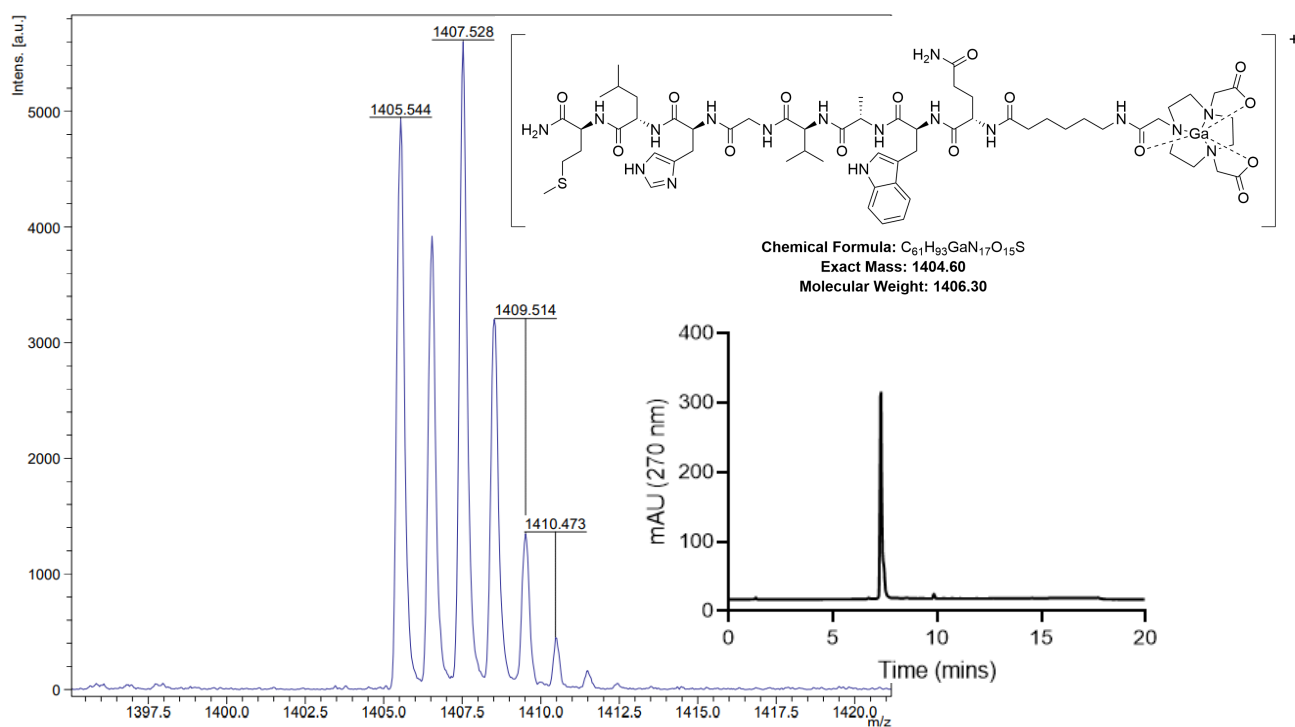


Figure S20. Characterization data for complex ^{nat}Ga-19.

Copper 2,2'-(7-((5*S*,8*S*,11*S*,17*S*,20*S*,23*S*,26*S*)-11-((1*H*-imidazol-4-yl)methyl)-23-((1*H*-indol-3-yl)methyl)-26-(3-amino-3-oxopropyl)-5-carbamoyl-8-isobutyl-17-isopropyl-20-methyl-7,10,13,16,19,22,25,28,35-nonaaxo-2-thia-6,9,12,15,18,21,24,27,34-nonaazahexatriacontan-36-yl)-1,4,7-triazonane-1,4-diyl)diacetate, (^{nat}Cu-19), Compound ^{nat}Cu-19 was synthesized using the generalized complexation procedure (Section 3.1) outlined in Scheme S4B followed by photocleavage (Section 2.5) from compound TG-Anp-19-^{nat}Cu. The product was isolated as a pale blue solid following deprotection and characterized using mass spectrometry and HPLC chromatography. Yield: (31 nmol, 31 %). R_t (Method A): 7.37 min. MALDI-MS [M+H]⁺ calc. for C₆₁H₉₃CuN₁₇O₁₅S 1399.6132, found 1399.447.

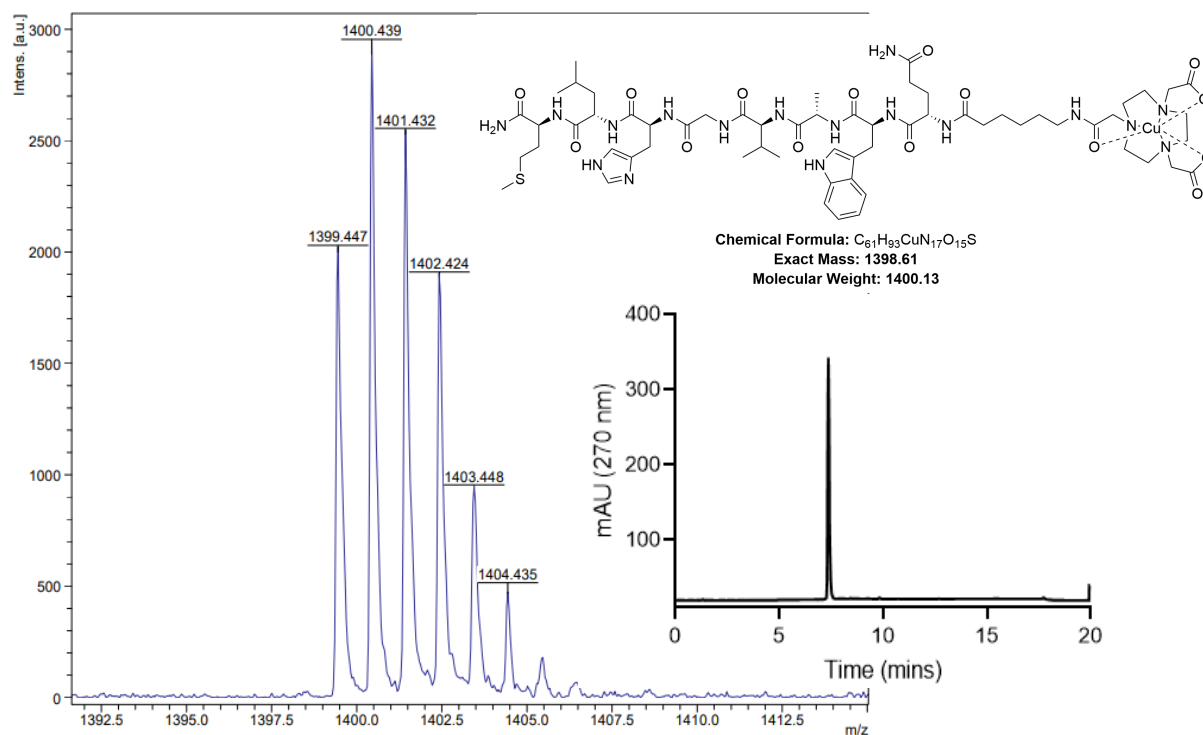


Figure S21. Characterization data for complex ^{nat}Cu-19.

Gallium (((1*S*)-5-(2-((1*S*,4*S*)-4-(((*S*)-2-(6-amino-6-oxohexanamido)-6-(2-(4,7-bis(carboxymethyl)-1,4,7-triazonan-1-yl)acetamido)hexanamido)methyl)cyclohexane-1-carboxamido)-3-(naphthalen-2-yl)propanamido)-1-carboxypentyl)carbamoyl)-*L*-glutamic acid bisacetate (^{nat}**Ga-31**). Compound ^{nat}**Ga-31** was synthesized using the generalized complexation procedure (Section 3.1) outlined in Scheme S4C followed by photocleavage (Section 2.5) from compound TG-Anp-31-^{nat}Ga. The product was isolated as a pale yellow solid following deprotection and characterized using mass spectrometry and HPLC chromatography. Yield: (29 nmol, 29 %). *R*_t (Method A): 7.78 min. MALDI-MS [*M*]⁺ calc. for C₅₇H₈₃GaN₁₁O₁₇ 1263.5302, found 1263.991.

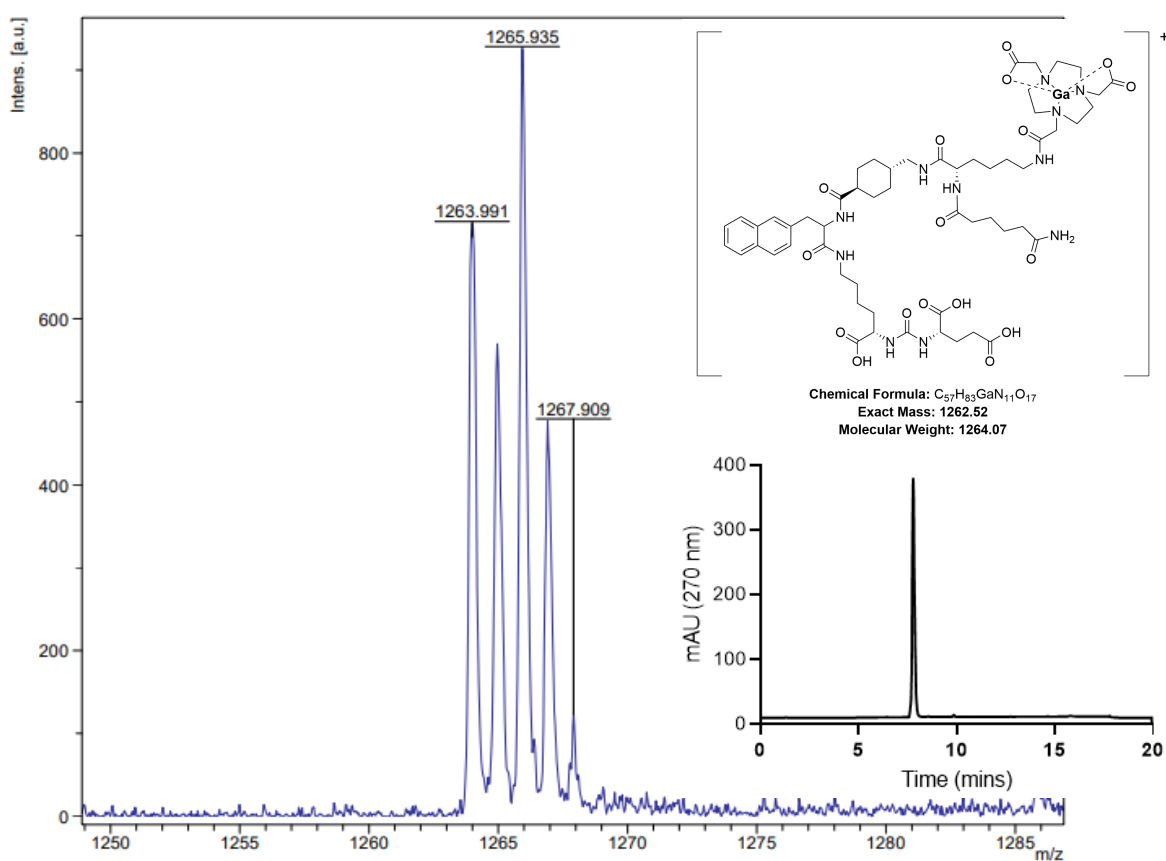


Figure S22. Characterization data for complex ^{nat}**Ga-31**.

Copper *(((1S)-5-(2-((1S,4S)-4-(((S)-2-(6-amino-6-oxohexanamido)-6-(2-(4,7-bis(carboxymethyl)-1,4,7-triazonan-1-yl)acetamido)hexanamido)methyl)cyclohexane-1-carboxamido)-3-(naphthalen-2-yl)propanamido)-1-carboxypentyl)carbamoyl)-L-glutamic acid bisacetate* (^{nat}Cu-31). Compound ^{nat}Cu-31 was synthesized using complexation procedure (Section 3.1) outlined in Scheme S4C followed by photocleavage (Section 2.5) from compound TG-Anp-31-^{nat}Cu. The product was isolated as a pale blue solid following deprotection and characterized using mass spectrometry and HPLC chromatography. Yield: (34 nmol, 34 %). R_t (Method A): 7.65 min. MALDI-MS [M+H]⁺ calc. for C₅₇H₈₃CuN₁₁O₁₇ 1257.5342, found 1256.720.

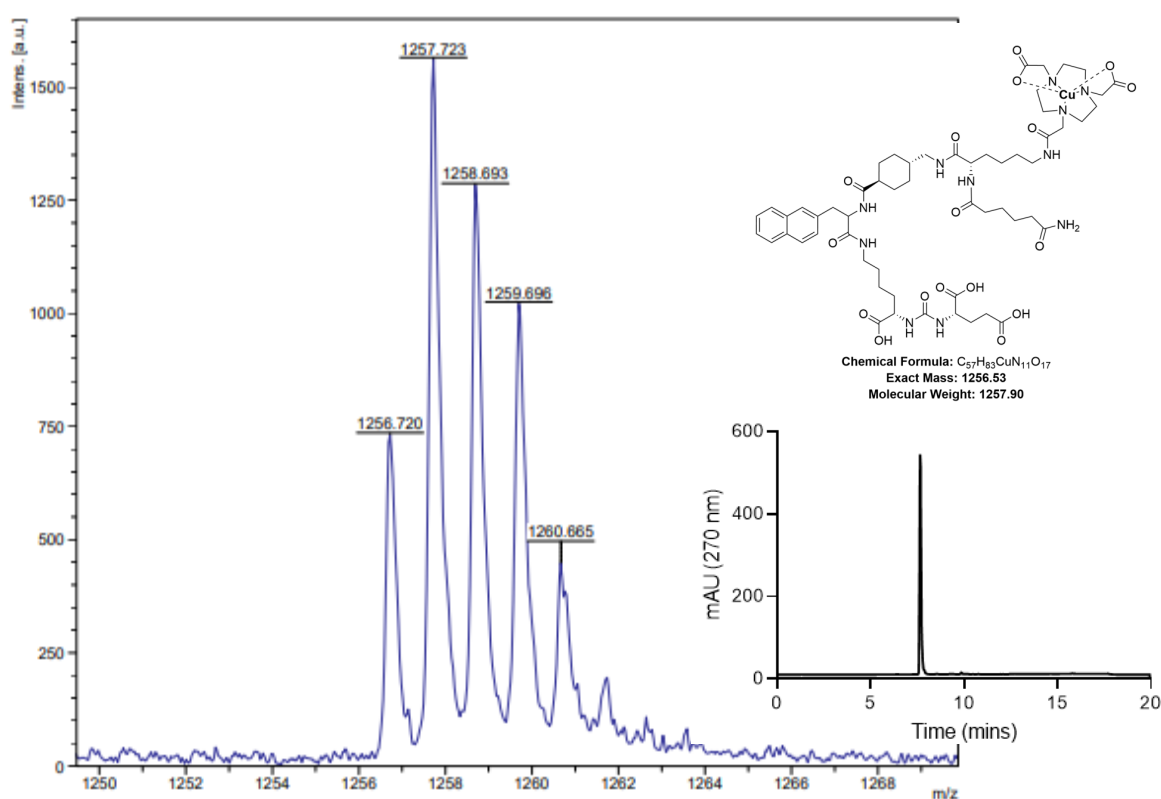


Figure S23. Characterization data for complex ^{nat}Cu-31.

4. NMR data

^1H NMR of **10** (400 MHz, D_2O) δ 7.67 (d, 1H), 7.49 (d, 1H), 7.25 (s, 2H), 7.16 (t, 1H), 4.68 (t, 1H), 4.18 (t, 1H), 3.87 (s, 4H), 3.68 (s, 2H), 3.32-3.09 (m, 16H), 2.19-2.11 (m, 4H), 1.91-1.81 (m, 2H), 1.49-1.43 (m, 4H), 1.24-1.20 (m, 2H).

^{13}C NMR of **10** (100 MHz, D_2O) δ 177.72, 177.10, 175.92, 173.06, 170.23, 162.74, 136.09, 126.87, 124.48, 121.98, 119.40, 118.29, 117.74, 114.84, 111.91, 108.79, 58.28, 56.15, 53.81, 53.25, 50.39, 49.82, 49.77, 39.35, 34.99, 30.84, 27.92, 26.84, 26.32, 25.51, 24.62.

^1H NMR of **Anp-10** (400 MHz, D_2O) δ 7.94 (d, 1H), 7.54-7.40 (m, 4H), 7.18 (t, 1H), 7.08 (t, 1H), 6.97-6.92 (m, 2H), 5.73 (t, 1H), 4.66 (t, 1H), 4.22 (t, 1H), 3.84 (s, 4H), 3.65 (s, 2H), 3.25-3.04 (m, 15H), 2.86-2.69 (m, 2H), 2.26-1.92 (m, 6H), 1.50-1.42 (m, 4H), 1.28-1.23 (m, 2H).

^{13}C NMR of **Anp-10** (100 MHz, D_2O) δ 177.72, 177.23, 173.76, 172.88, 172.18, 171.89, 170.16, 163.08, 162.73, 147.27, 135.98, 135.04, 134.30, 128.85, 127.66, 126.60, 124.84, 124.28, 121.93, 120.65, 119.35, 118.07, 117.74, 114.84, 111.99, 108.01, 58.29, 56.08, 54.11, 53.46, 50.32, 49.77, 45.88, 39.39, 39.12, 34.97, 30.95, 27.95, 26.92, 26.45, 25.55, 24.59.

^1H NMR of $^{\text{nat}}\text{Ga-10}$ (400 MHz, D_2O) δ 7.69 (d, 1H), 7.50 (d, 1H), 7.26 (s, 2H), 7.18 (t, 1H), 4.69 (t, 1H), 4.19 (s, 3H), 3.85 (s, 3H), 3.49-3.09 (m, 14H), 2.18-2.14 (m, 4H), 1.90-1.81 (m, 7H), 1.59-1.43 (m, 4H), 1.25-1.19 (m, 2H).

^{13}C NMR of $^{\text{nat}}\text{Ga-10}$ (100 MHz, D_2O) δ 180.98, 177.73, 176.97, 175.96, 174.50, 173.13, 172.16, 136.12, 126.87, 124.49, 121.99, 119.40, 118.30, 119.92, 108.83, 61.91, 59.75, 53.76, 53.31, 53.27, 53.16, 53.11, 41.61, 34.83, 30.87, 26.97, 26.81, 26.32, 25.22, 24.32, 22.94.

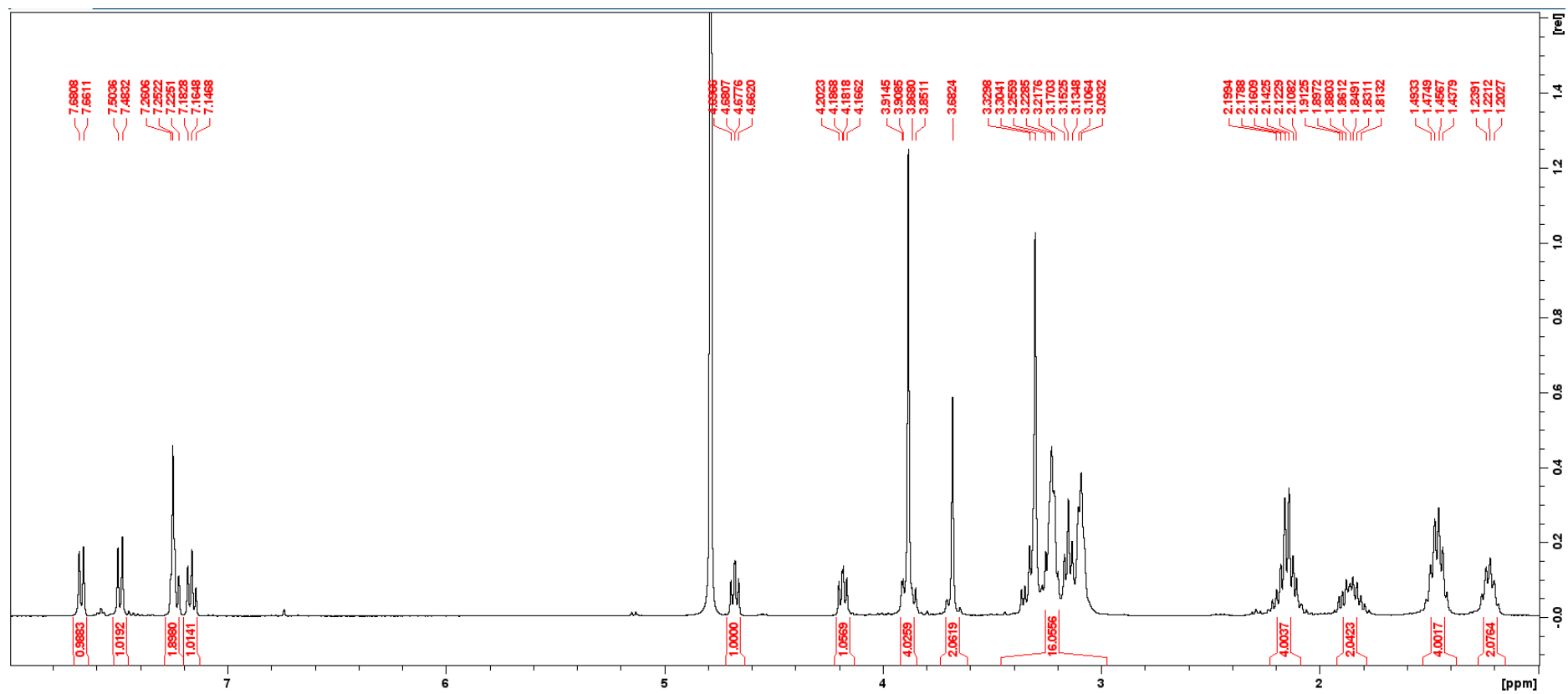


Figure S24. ¹H NMR of compound **10**. 400 MHz, D₂O.

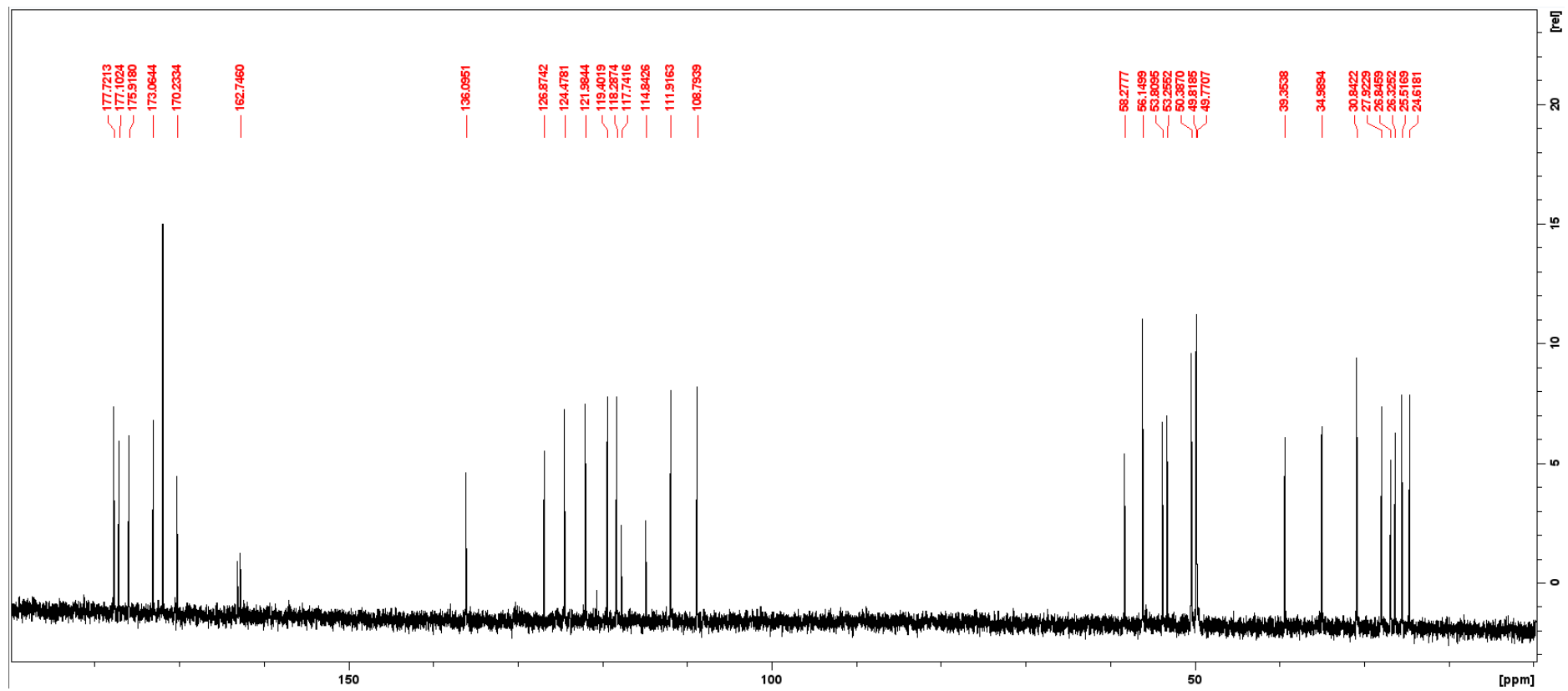


Figure S25. ^{13}C NMR of compound 10. 100 MHz, D_2O .

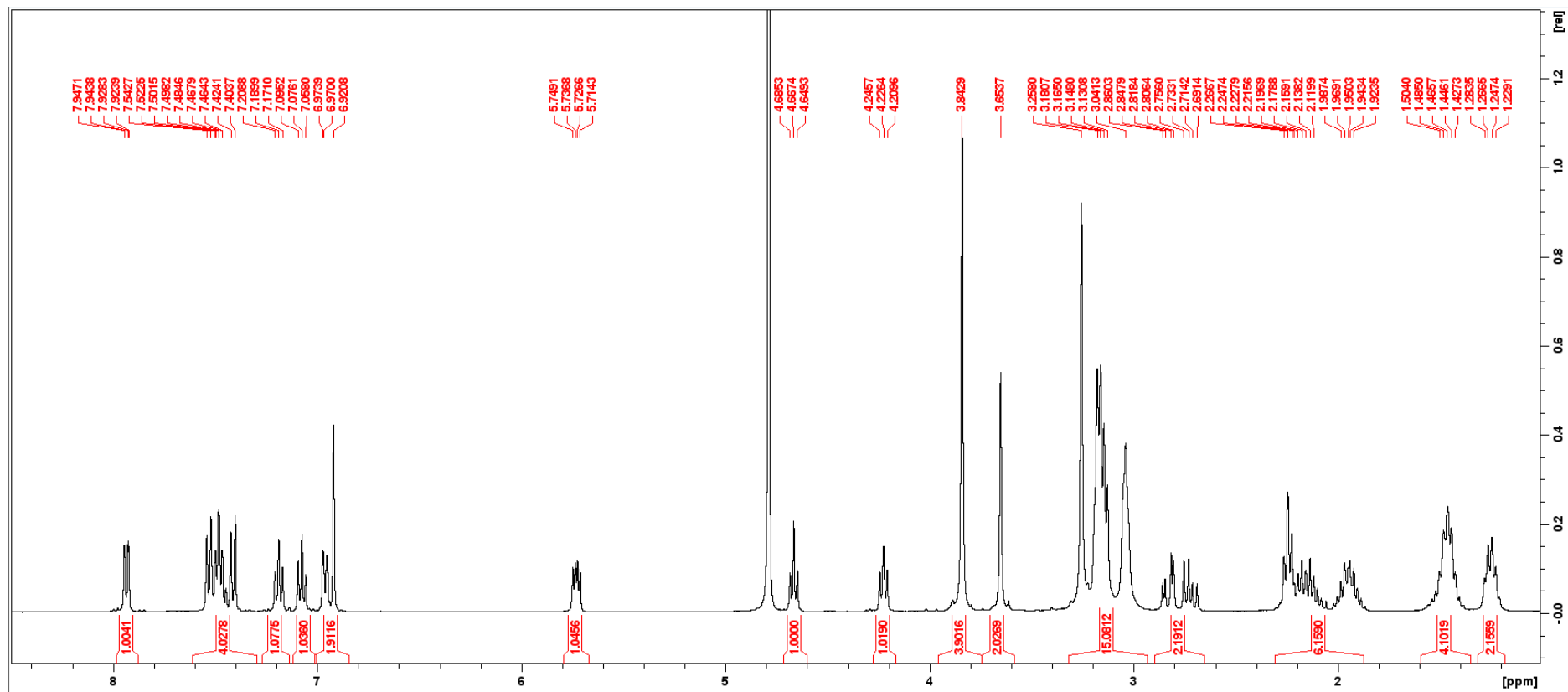


Figure S26. ¹H NMR of compound Anp-10. 400 MHz, D₂O.

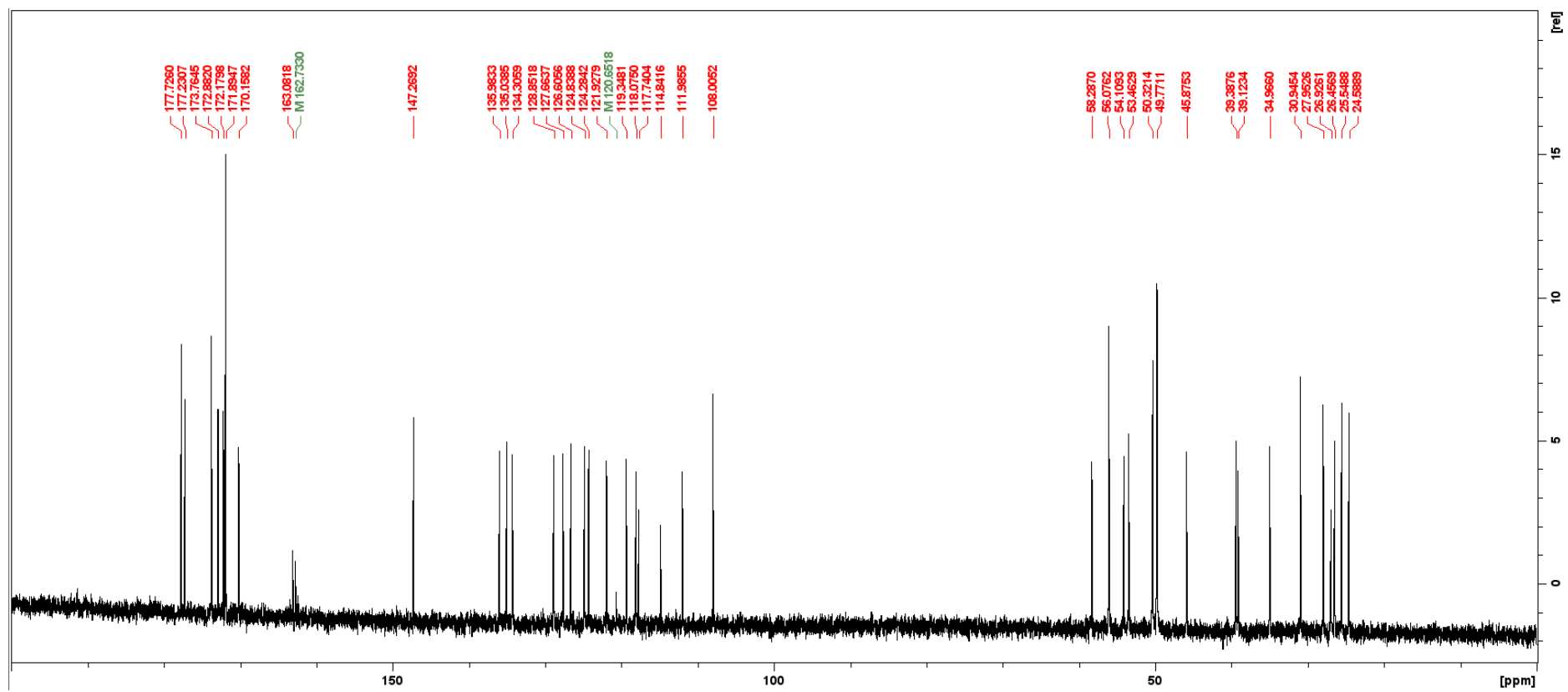


Figure S27. ^{13}C NMR of compound Anp-10. 100 MHz, D_2O .

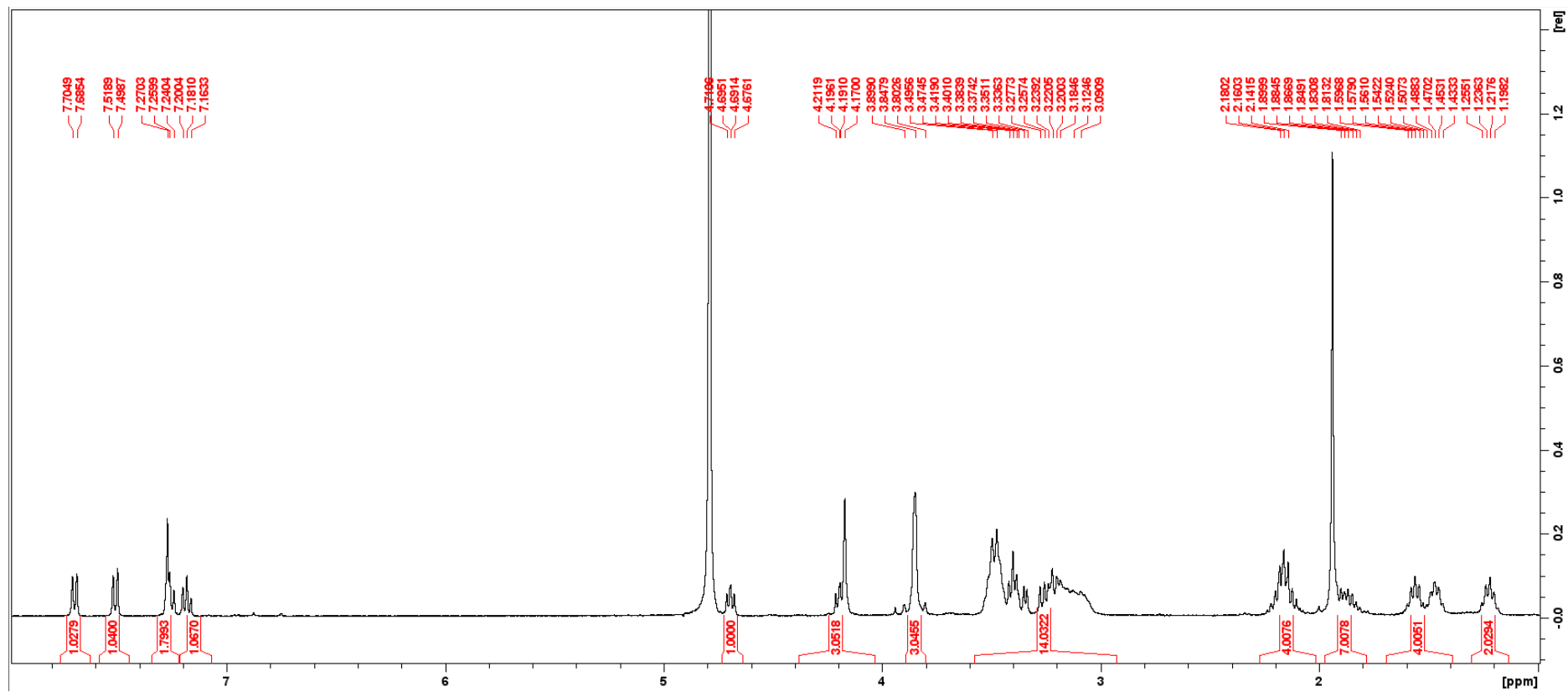


Figure S28. ^1H NMR of compound $^{\text{nat}}\text{Ga-10}$. 400 MHz, D_2O .

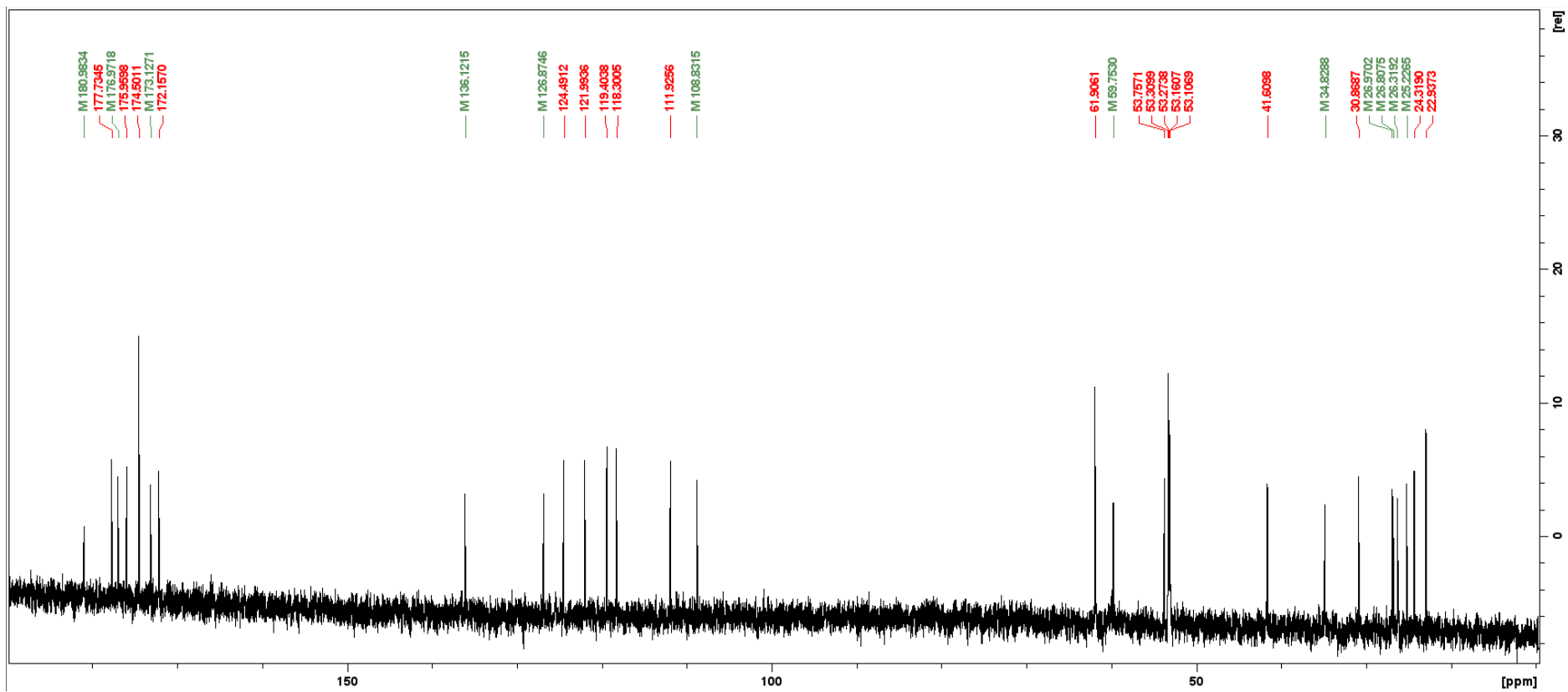
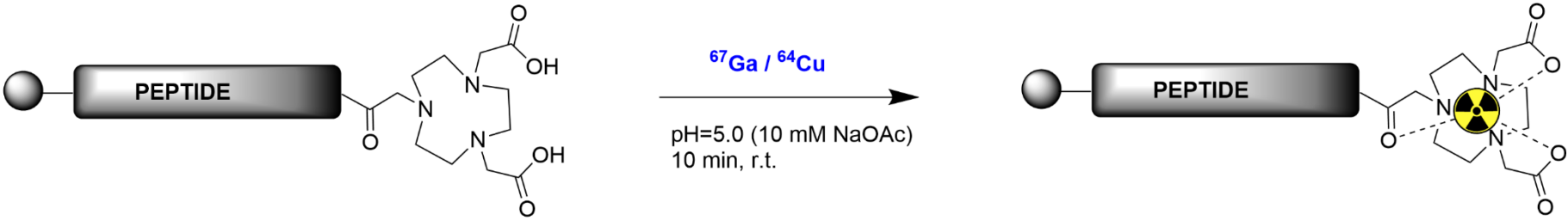


Figure S29. ^{13}C NMR of compound $^{\text{nat}}\text{Ga-10}$. 100 MHz, D_2O .

5. Synthesis and Characterization of Radiochemical Complexes

Table S2. Radiolabeling reaction and data.



Peptide	Isotope	SA [$\mu\text{Ci/nmol}$]	RCY [%]	RCP [%]
BBN (19)	^{67}Ga	5.0	90.0	99.9
PSMA (31)	^{67}Ga	5.0	85.5	99.9
BBN (19)	^{64}Cu	5.1	89.8	99.8
PSMA (31)	^{64}Cu	5.1	88.8	99.8

5.1 General radiolabeling protocol

5.1.1 Resin preparation

The resin-bound peptide, NOTA-Aca-BBN (0.1 mg, 10 nmol) or NOTA-PSMA (0.4 mg, 10 nmol), was washed with 3 mL of DCM, DMF, H₂O and 10 mM NaOAc buffer (pH=5.0) three times each for 1 min. The resin was stored in 10 mM of sodium acetate (NaOAc) buffer until use.

5.1.2 Radiolabeling with ⁶⁷Ga.

⁶⁷Ga-citrate was purchased from Jubilant Radiopharma at an average specific activity of 5.0 mCi/mL. The ⁶⁷Ga-citrate solution was first converted to ⁶⁷GaCl₃ using an established solid-phase extraction protocol.⁶ The resulting average specific activity of the obtained ⁶⁷Ga-chloride solution used for solid-phase radio-labeling was 1.1 mCi/mL. For radio-labeling of NOTA-Aca-BBN (**19**) or NOTA-PSMA (**31**), a 10 μL aliquot containing 50 μCi of ⁶⁷GaCl₃ was added to the resin-bound conjugate (10 nmol, 300 μL) in 10 mM of sodium acetate (NaOAc) buffer. The pH of the solution was adjusted to 5.0. Radiolabeling was completed after 20 minutes at room temperature. The radiolabeled conjugates were photocleaved for 10 min and characterized with radio-HPLC. ⁶⁷Ga-**19**: R_t = 7.28 min (purity/peak area: 99.9%). ⁶⁷Ga-**31**: R_t = 7.43 min (purity/peak area: 99.0%).

5.1.3 Radiolabeling with ⁶⁴Cu.

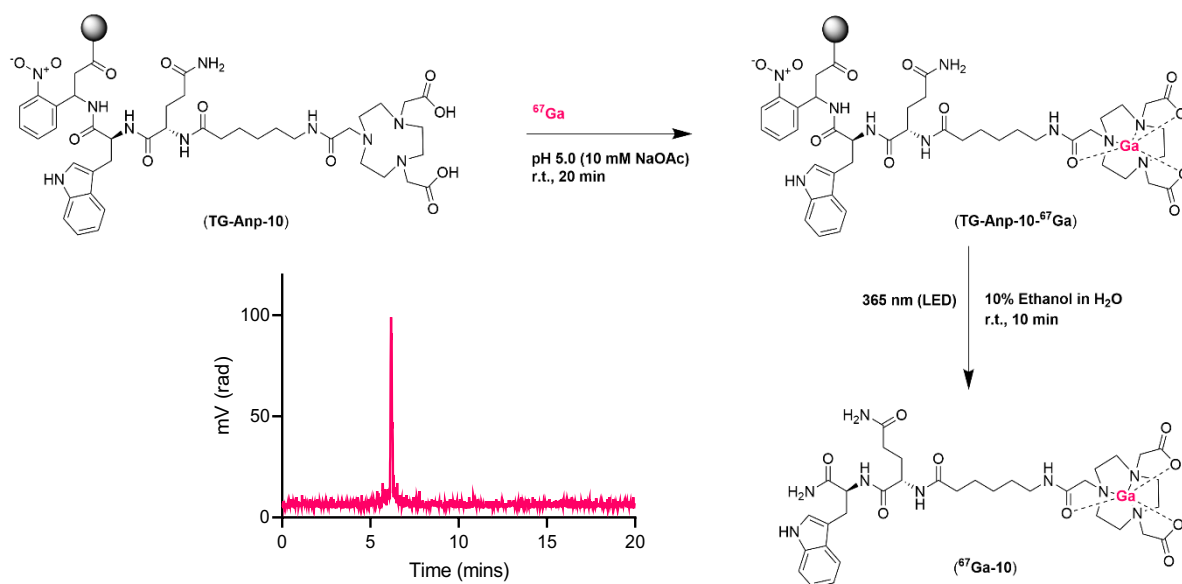
The ⁶⁴Cu isotope stock solution (copper-64 chloride, pH=2) was produced at the University of Wisconsin-Madison, Medical Physics Dept., Madison, WI. The ⁶⁴Cu-chloride was obtained at an average specific activity of 0.23 mCi/μL. For radiolabeling of NOTA-Aca-BBN (**19**) or NOTA-PSMA (**31**), a 15 μL aliquot containing 50 μCi of ⁶⁴CuCl₂ was added to the resin-bound ligand (10 nmol, 300 μL) in 10 mM of sodium acetate (NaOAc) buffer. The pH of the solution was adjusted to 5.0. Radiolabeling was completed within 20 minutes at room temperature. The radiolabeled conjugates were photocleaved for 10 min and characterized with radio-HPLC. ⁶⁴Cu-**19**: R_t = 7.42 min (purity/peak area: 98.0%). ⁶⁴Cu-**31**: R_t = 7.65 min (purity/peak area: 99.0%).

5.1.4 Radiolabeling with ⁶⁸Ga.

⁶⁸Ga-chloride was obtained from an Eckhard & Ziegler ⁶⁸Ge/⁶⁸Ga generator (30 mCi), housed in the department of Radiology, Stony Brook University, Stony Brook, New York, at an average specific activity of 10 mCi/mL. For radio-labeling of NOTA-PSMA, a 1.0 mL aliquot containing 2.0 mCi of ⁶⁸GaCl₃ was added to the resin-bound conjugate (10 nmol, 300 μL) in 1.0 M of sodium acetate (NaOAc) buffer. The pH of the solution was adjusted to 5.0. Radiolabeling was completed after 20 minutes at room temperature. The radiolabeled conjugate was photocleaved for 10 min and characterized with radio-HPLC. ⁶⁸Ga-**31**: R_t = 7.40 min (purity/peak area: 99%).

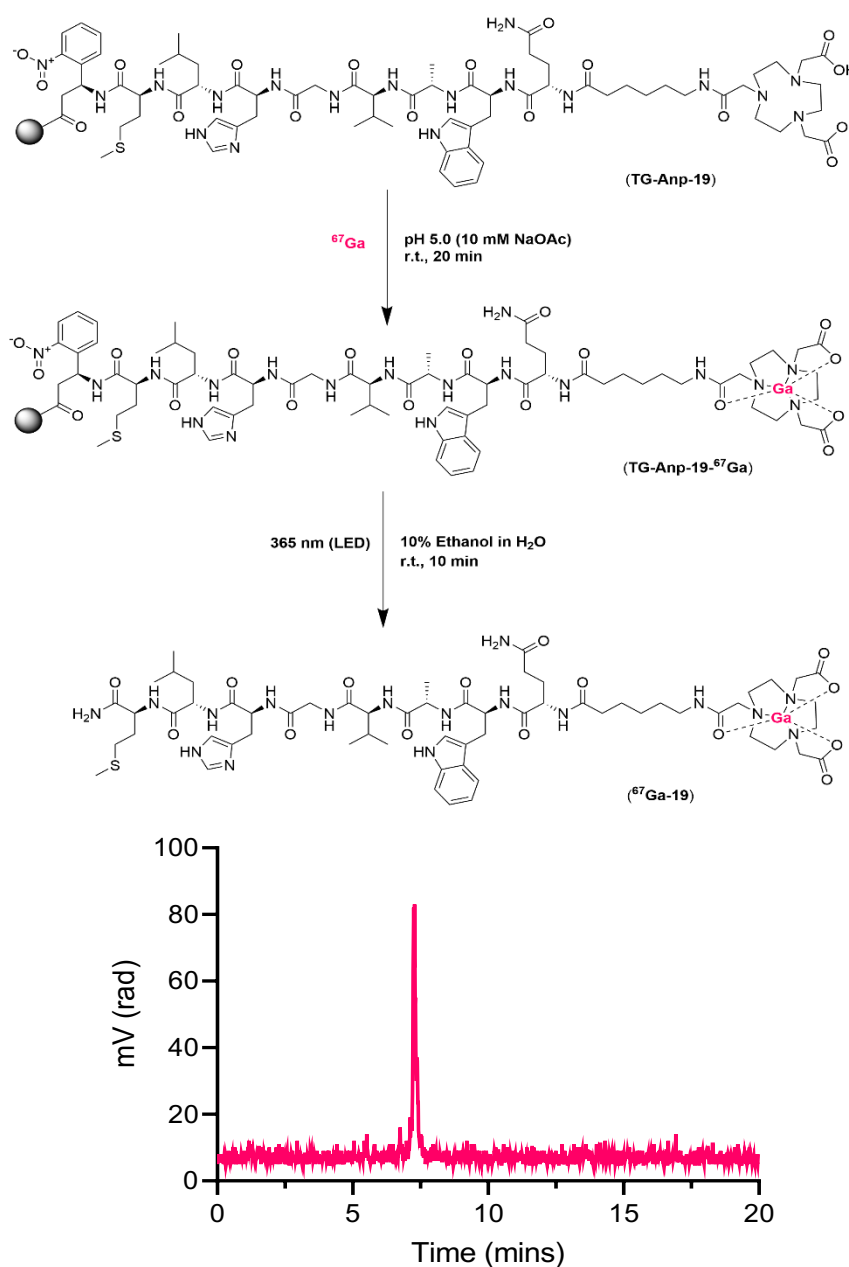
5.2 Synthesis of ^{67}Ga -radiolabeled complexes

^{67}Ga Gallium 2,2'-(7-((5*S*,8*S*)-5-((1*H*-indol-3-yl)methyl)-8-(3-amino-3-oxopropyl)-1-carboxy-2-(2-nitrophenyl)-4,7,10,17-tetraoxo-3,6,9,16-tetrazaoctadecan-18-yl)-1,4,7-triazonane-1,4-diyl)diacetate ($^{67}\text{Ga-10}$). Compound $^{67}\text{Ga-10}$ was synthesized using the general radiolabeling protocol followed by photocleavage from intermediate **TG-Anp-10- ^{67}Ga** . The product was isolated by direct filtration-mediated removal of the resin support and characterized using radio-HPLC chromatography. R_t (Method C): 6.20 min. SA: 5.0 $\mu\text{Ci/nmol}$, RY: 95.0 %, RCY: 55 %, RCP: 99 %.



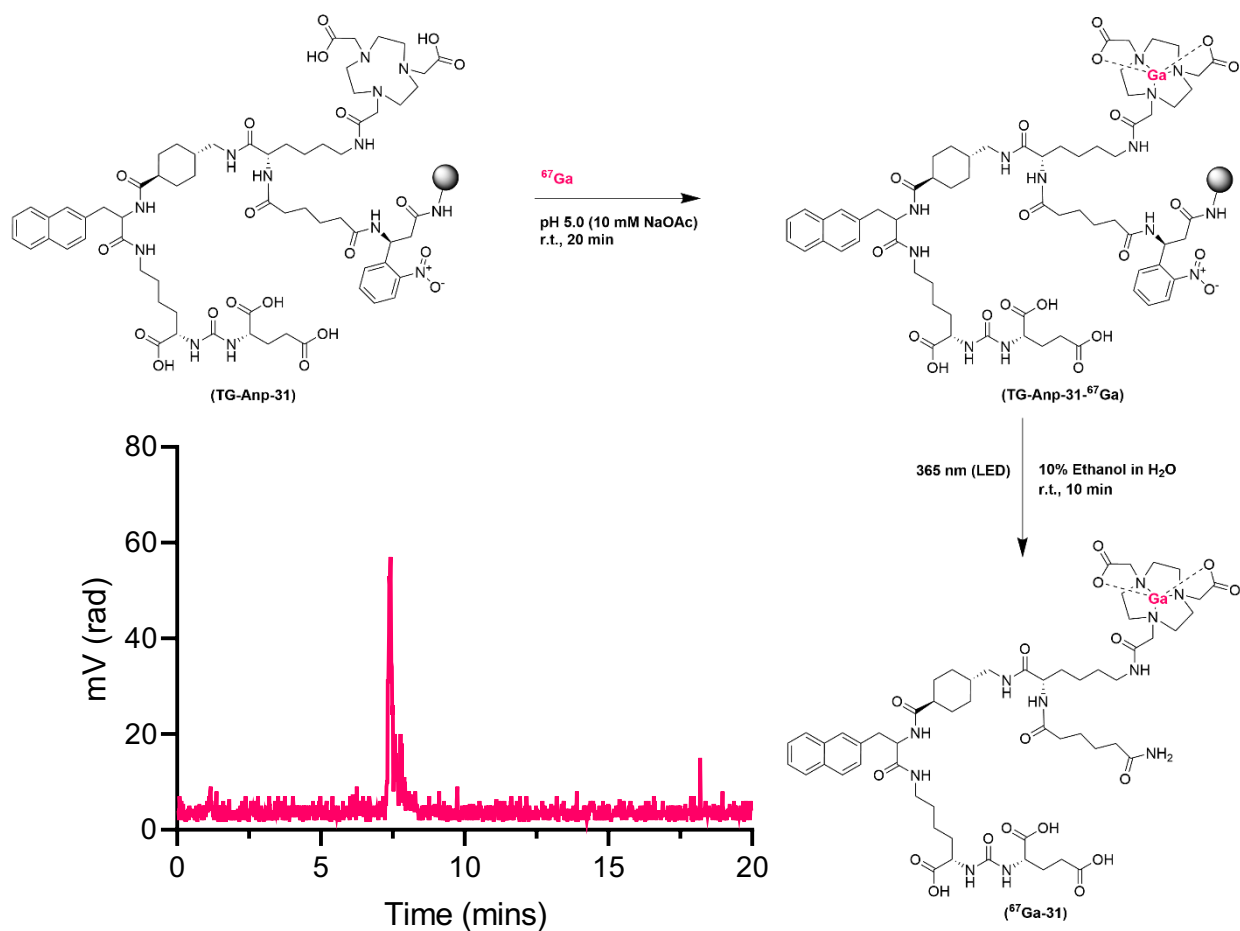
Scheme S5. Reaction scheme and corresponding radio-HPLC trace.

⁶⁷Gallium 2,2'-(7-((5*S*,8*S*,11*S*,17*S*,20*S*,23*S*,26*S*)-11-((1*H*-imidazol-4-yl)methyl)-23-((1*H*-indol-3-yl)methyl)-26-(3-amino-3-oxopropyl)-5-carbamoyl-8-isobutyl-17-isopropyl-20-methyl-7,10,13,16,19,22,25,28,35-nonaoxo-2-thia-6,9,12,15,18,21,24,27,34-nonaazahexatriacontan-36-yl)-1,4,7-triazonane-1,4-diyl)acetate (⁶⁷Ga-19). Compound ⁶⁷Ga-31 was synthesized using the general radiolabeling protocol followed by photocleavage from intermediate TG-Anp-19-⁶⁷Ga. The product was isolated by direct filtration-mediated removal of the resin support and characterized using radio-HPLC chromatography. R_t (Method C): 7.28 min. SA: 5.0 μCi/nmol, RY: 90.0 %, RCY: 40.0 %, RCP: 99.9 %.



Scheme S6. Reaction scheme and corresponding radio-HPLC trace.

^{67}Ga of (((1*S*)-5-(2-(((1*S*,4*S*)-4-(((*S*)-2-(6-amino-6-oxohexanamido)-6-(2-(4,7-bis(carboxymethyl)-1,4,7-triazonan-1-yl)acetamido)hexanamido)methyl)cyclohexane-1-carboxamido)-3-(naphthalen-2-yl)propanamido)-1-carboxypentyl)carbonyl)-*L*-glutamic acid bisacetate (^{67}Ga -31). Compound ^{67}Ga -31 was synthesized using the general radiolabeling protocol followed by photocleavage from intermediate **TG-Anp-31- ^{67}Ga** . The product was isolated by direct filtration-mediated removal of the resin support and characterized using radio-HPLC chromatography. R_t (Method C): 7.43 min. SA: 5.1 $\mu\text{Ci/nmol}$, RY: 92.0 %, RCY: 45.5 %, RCP: 99.0 %.



Scheme S7. Reaction scheme and corresponding radio-HPLC trace.

5.2.1 Representative radiolabeling traces of NOTA-Aca-BBN (**19**).

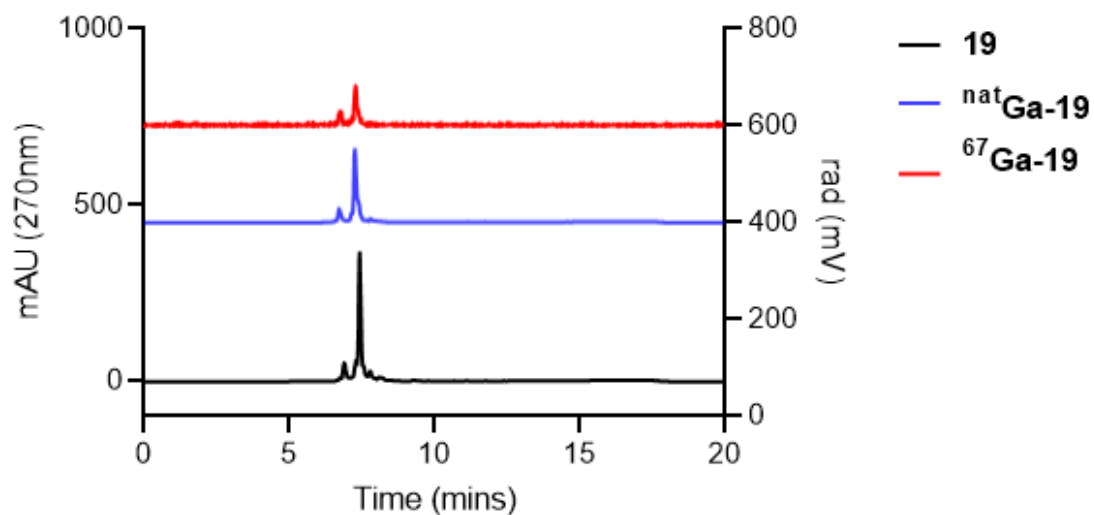


Figure S30. HPLC chromatograms (method C, UV trace recorded at 270 nm) and radio-HPLC chromatogram of **19** and its oxidized side product.

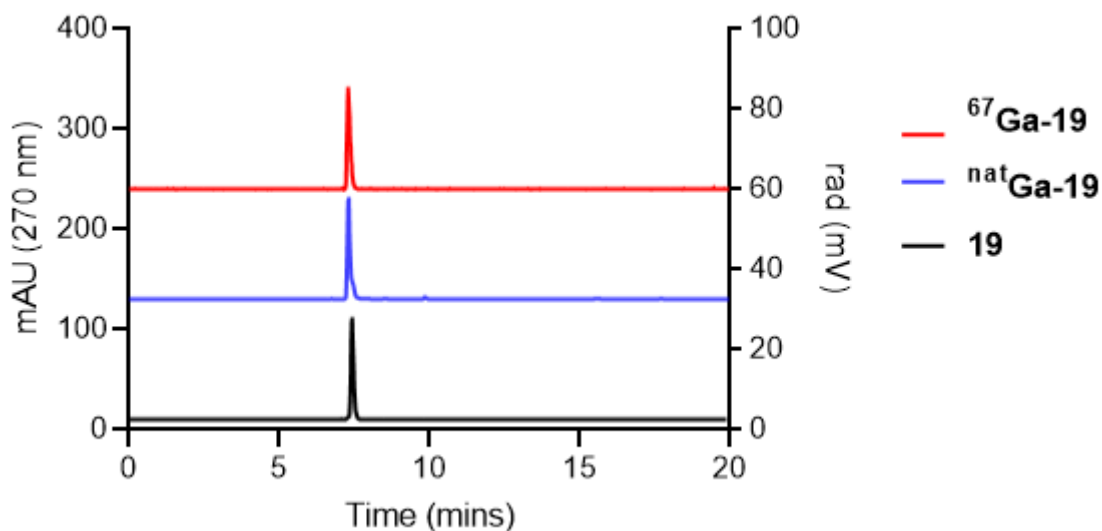


Figure S31. HPLC chromatograms (method C, UV trace recorded at 270 nm) and corresponding radio-HPLC chromatogram of **19** (after optimized deprotection).

5.2.2 Representative radiolabeling traces of NOTA-PSMA (31).

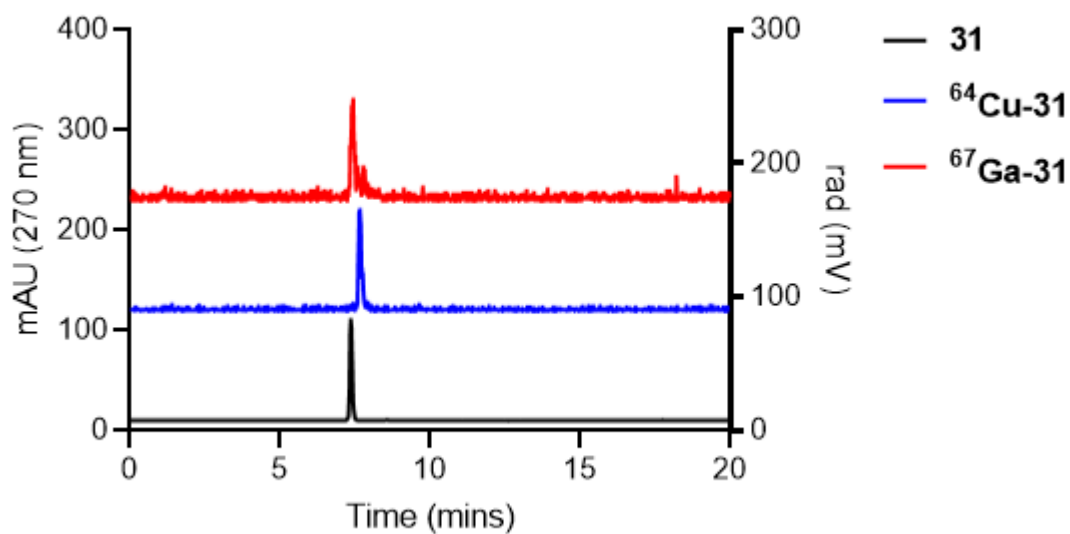


Figure S32. HPLC chromatograms (method C, UV trace recorded at 270 nm) and corresponding radio-HPLC chromatogram of ⁶⁷Ga-31.

5.2.3 Concentration-dependent Radiolabeling

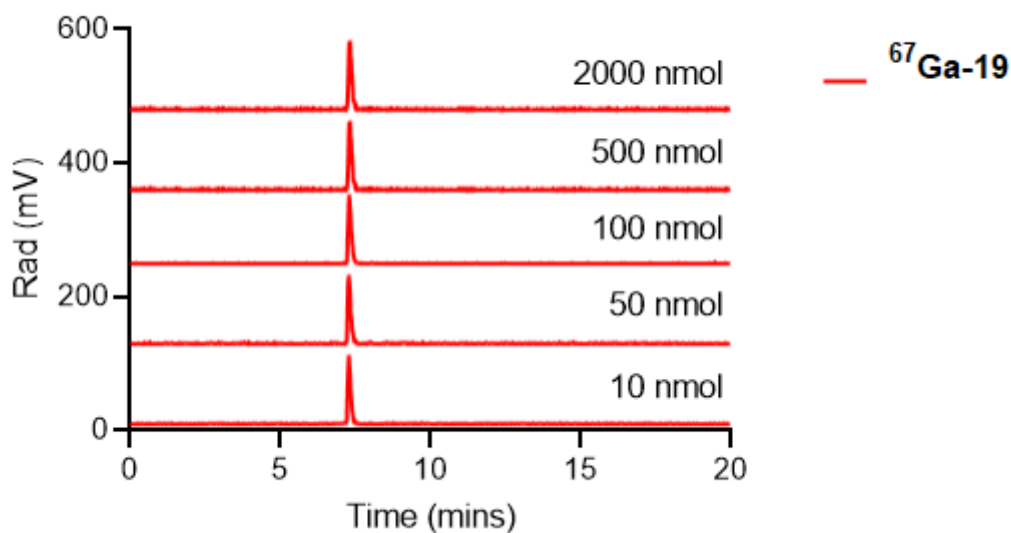


Figure S33. Radio-HPLC chromatogram of concentration-dependent radiolabeling for ⁶⁷Ga-19.

5.2.4 Volume-dependent radiolabeling

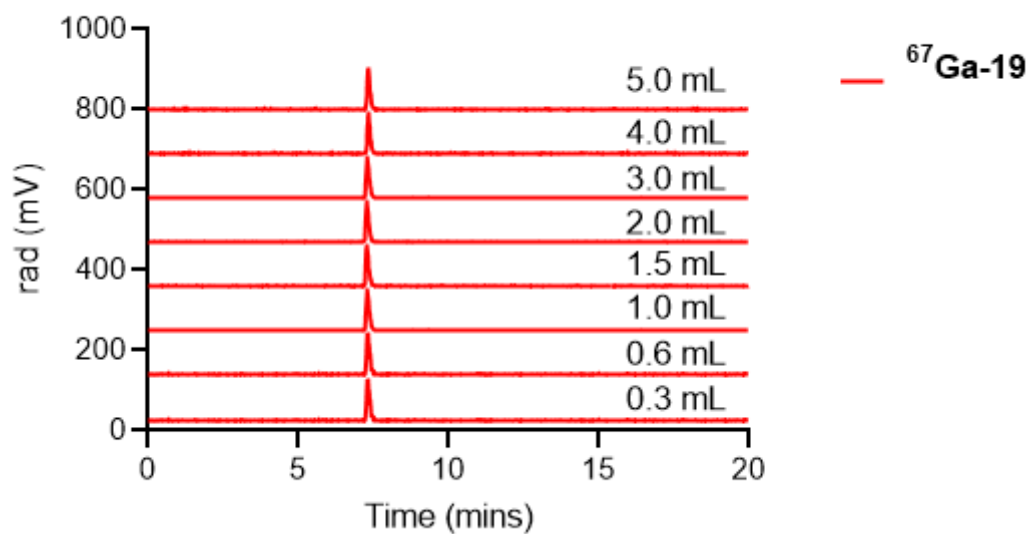


Figure S34. Radio-HPLC chromatograms (normalized) of volume-dependent radiolabeling reaction on solid phase for $^{67}\text{Ga-19}$.

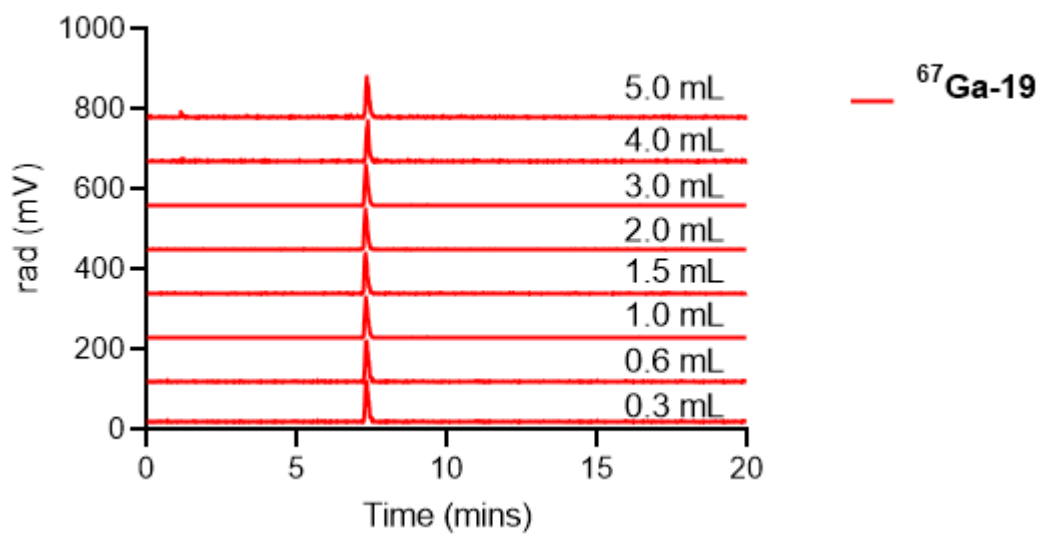


Figure S35. Radio-HPLC chromatograms (normalized) of volume-dependent radiolabeling reaction in solution for $^{67}\text{Ga-19}$.

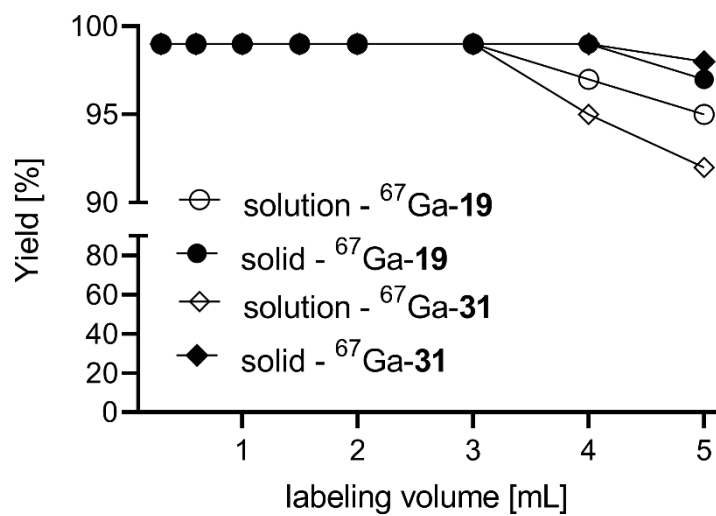


Figure S36. The radiochemical yields showing the best performance for large volumes for the resin-based method (“solid”) in comparison to radiolabeling in solution (“solution”) where yields decline above 4 mL reaction volumes

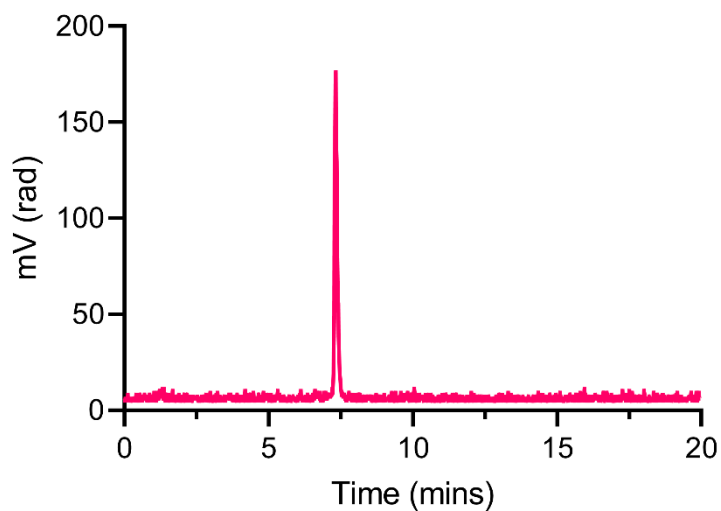
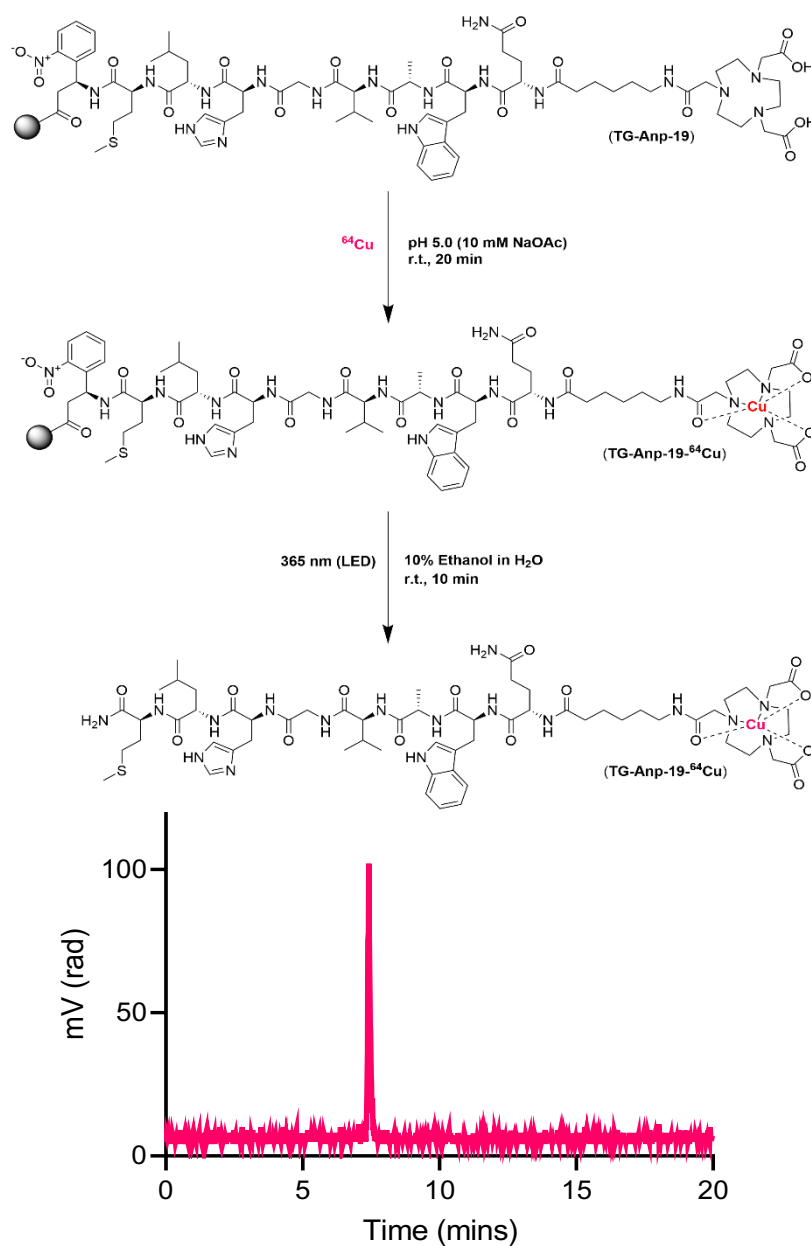


Figure S37. Radio-HPLC chromatogram of ⁶⁷Ga-19 using immobilized-resin stored at 4 °C for 6 months.(no degradation products present).

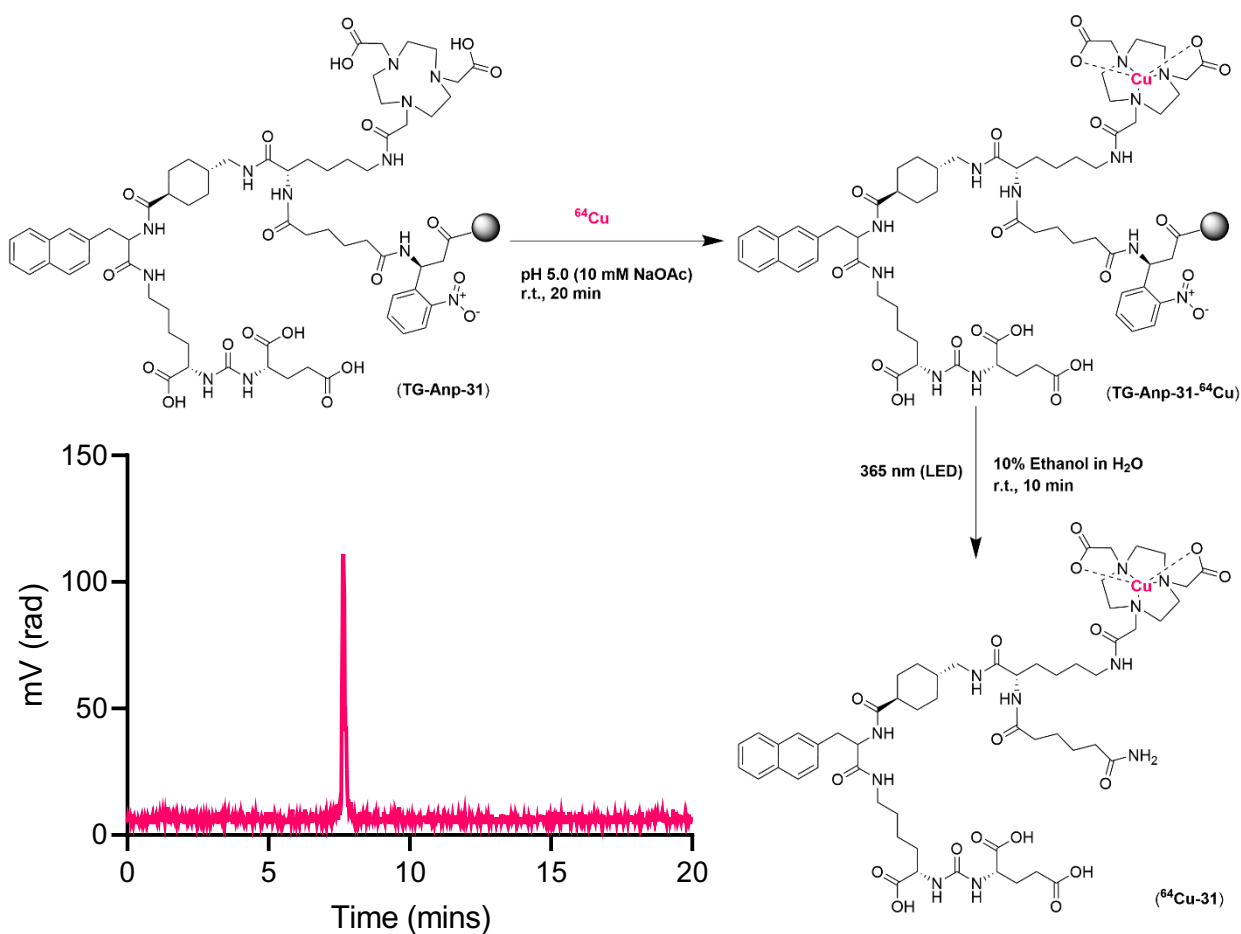
5.3 Synthesis of ^{64}Cu -radiolabeled complexes

$^{64}\text{Copper}$ 2,2'-((7-((5*S*,8*S*,11*S*,17*S*,20*S*,23*S*,26*S*)-11-((1*H*-imidazol-4-yl)methyl)-23-((1*H*-indol-3-yl)methyl)-26-(3-amino-3-oxopropyl)-5-carbamoyl-8-isobutyl-17-isopropyl-20-methyl-7,10,13,16,19,22,25,28,35-nonaoxo-2-thia-6,9,12,15,18,21,24,27,34-nonaazahexatriacontan-36-yl)-1,4,7-triazonane-1,4-diyl)diaceticate (^{64}Cu -**19**). Compound ^{64}Cu -**19** was synthesized using general radiolabeling protocol followed by photocleavage from intermediate **TG-Anp-19- ^{64}Cu** . The product was isolated by direct filtration-mediated removal of the resin support and characterized using radio-HPLC chromatography. R_t (Method C): 7.42 min. SA: 5.0 $\mu\text{Ci}/\text{nmol}$, RY: 88.0 %, RCY: 48.0 %, RCP: 98.0 %.



Scheme S8. Reaction scheme and corresponding radio-HPLC trace.

⁶⁴Copper (((1*S*)-5-(2-((1*S*,4*S*)-4-(((*S*)-2-(6-amino-6-oxohexanamido)-6-(2-(4,7-bis(carboxymethyl)-1,4,7-triazonan-1-yl)acetamido)hexanamido)methyl)cyclohexane-1-carboxamido)-3-(naphthalen-2-yl)propanamido)-1-carboxypentyl)carbamoyl)-*L*-glutamic acid diacetate (⁶⁴Cu-31). Compound ⁶⁴Cu-31 was synthesized using general radiolabeling protocol followed by photocleavage strategy from intermediate **TG-Anp-31-⁶⁴Cu**. The product was isolated by direct filtration-mediated removal of the resin support and characterized using radio-HPLC chromatography. R_t (Method C): 7.65 min. SA: 5.1 μCi/nmol, RY: 88.0 %, RCY: 44.0 %, RCP: 99.0 %.



Scheme S9. Reaction scheme and corresponding radio-HPLC trace.

5.3.1 Representative radiolabeling traces of NOTA-Aca-BBN (19)

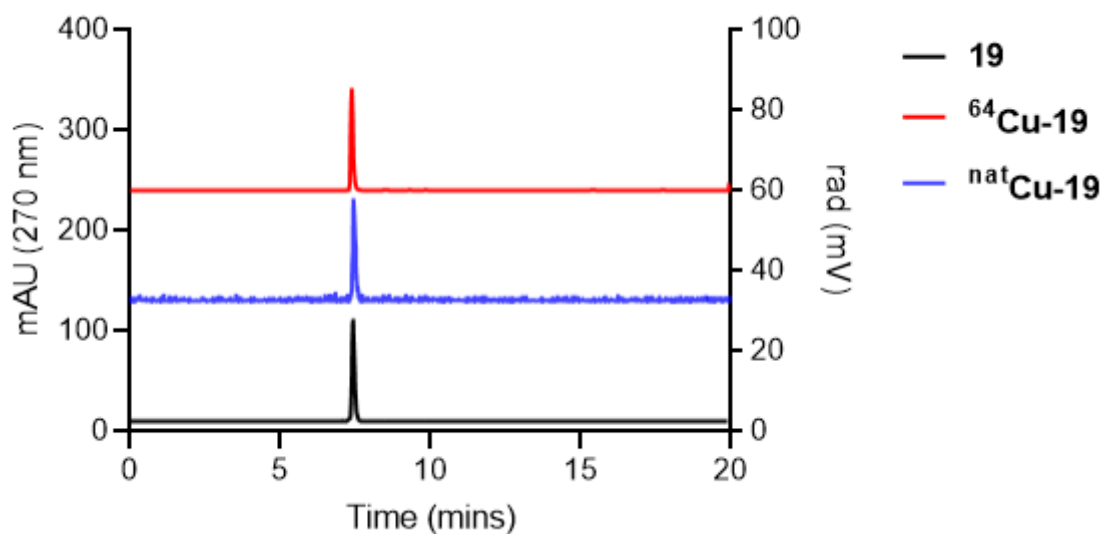


Figure S38. HPLC chromatograms (method C, UV trace recorded at 270 nm) and corresponding radio-HPLC chromatogram of $^{64}\text{Cu-19}$.

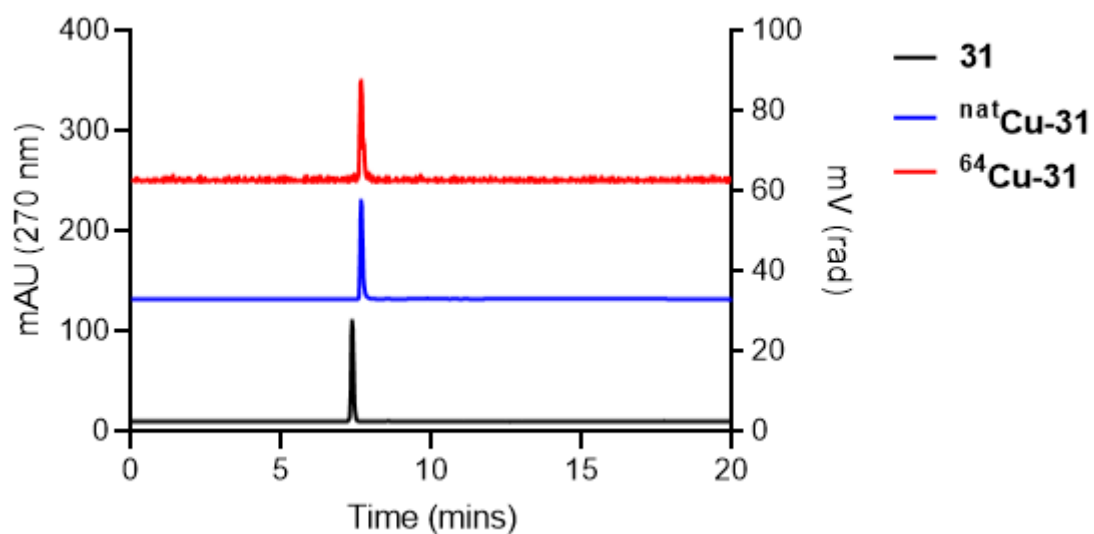


Figure S39. HPLC chromatograms (method C, UV trace recorded at 270 nm) and corresponding radio-HPLC chromatogram of $^{64}\text{Cu-31}$.

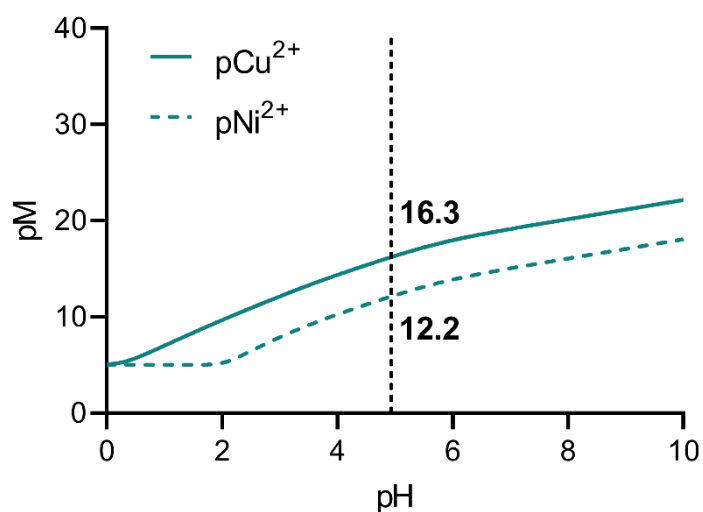


Figure S40. The pH dependence of relative pM values of NOTA for Cu²⁺ and Ni²⁺; at radiolabeling pH, pM values are 16.3 (pCu) and 12.2 (pNi) respectively.

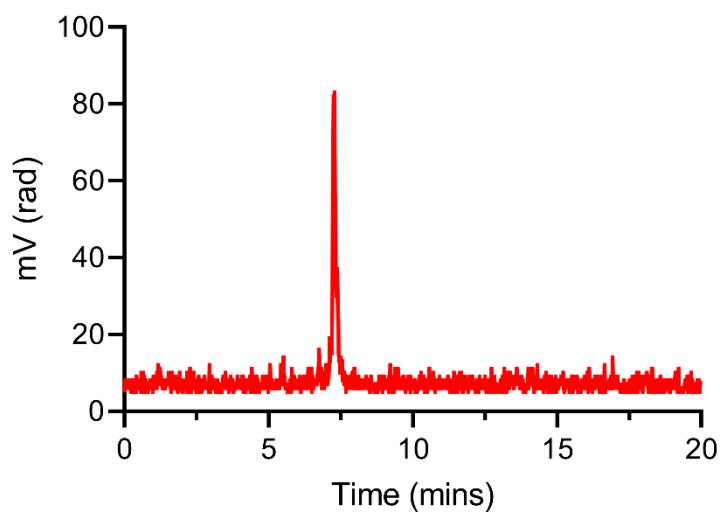
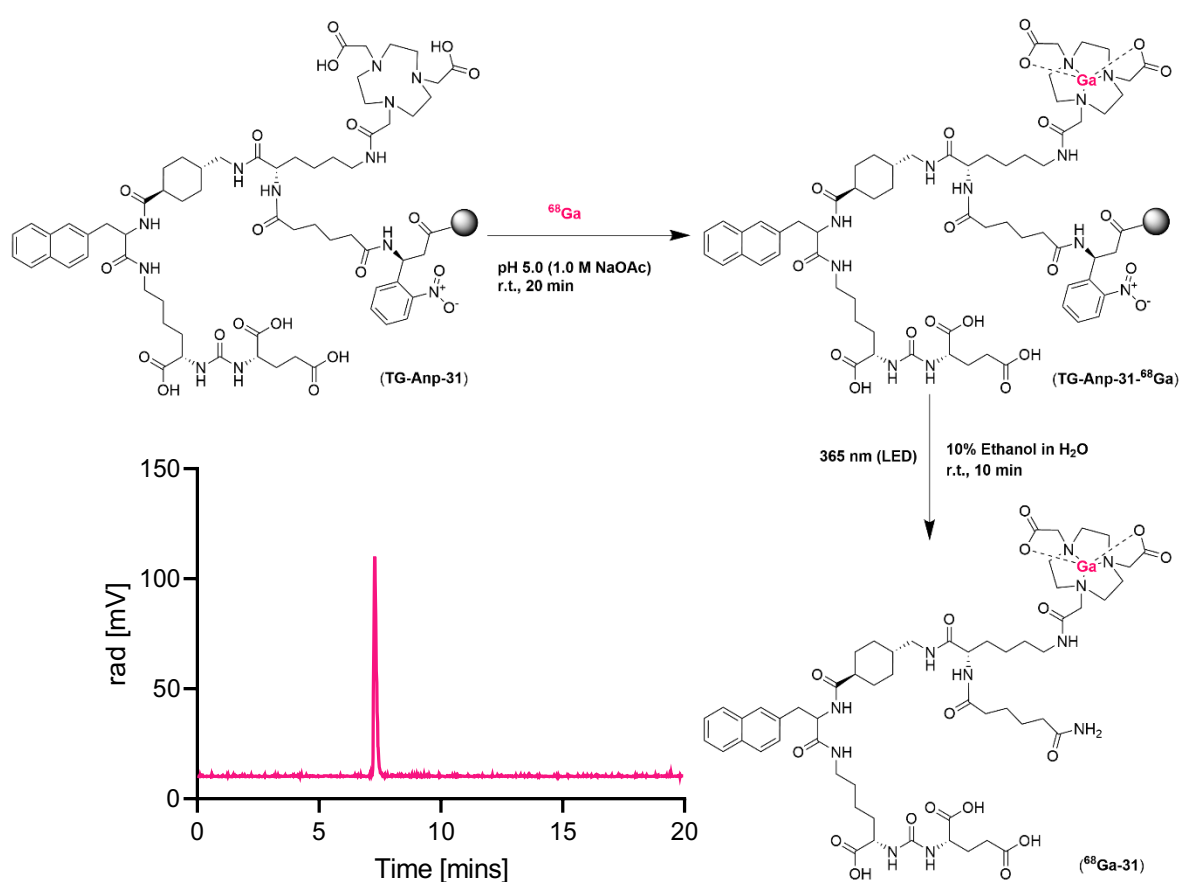


Figure S41. Radio-HPLC chromatogram of ⁶⁷Ga-19 for the SPRP synthesis of ⁶⁷Ga-19 in presence of non-radioactive ^{nat}Zn carrier.

5.4 Synthesis of ^{68}Ga -radiolabeled complex

^{68}Ga of *((1S)-5-(2-((1S,4S)-4-(((S)-2-(6-amino-6-oxohexanamido)-6-(2-(4,7-bis(carboxymethyl)-1,4,7-triazonan-1-yl)acetamido)hexanamido)methyl)cyclohexane-1-carboxamido)-3-(naphthalen-2-yl)propanamido)-1-carboxypentyl)carbamoyl)-L-glutamic acid bisacetate (^{68}Ga -31). Compound ^{68}Ga -31 was synthesized using the general radiolabeling protocol followed by photocleavage from intermediate **TG-Anp-31- ^{68}Ga** . The product was isolated by direct filtration-mediated removal of the resin support and characterized using radio-HPLC chromatography. R_t (Method C): 7.40 min. SA: 0.2 mCi/nmol, RY: 98 %, RCY: 40 %, RCP: 99.0 %.*



Scheme S10. Reaction scheme and corresponding radio-HPLC trace of ^{68}Ga -31.

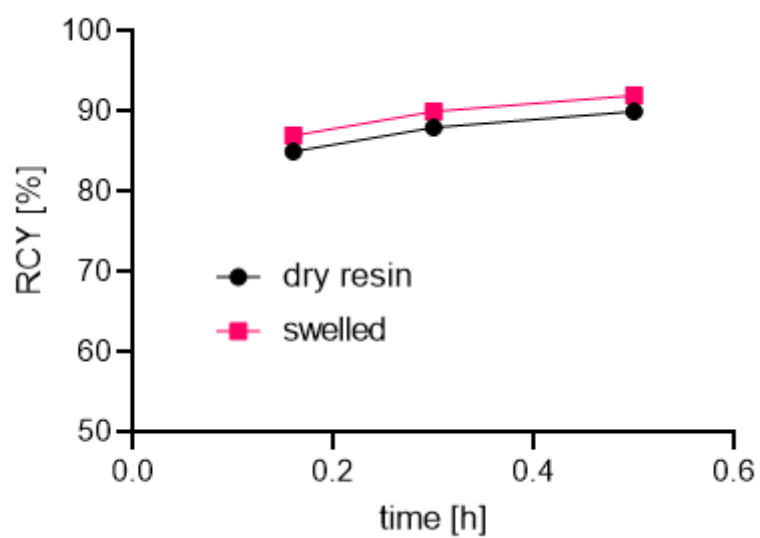


Figure S42. Radiolabeling yields for dry vs. swelled resin

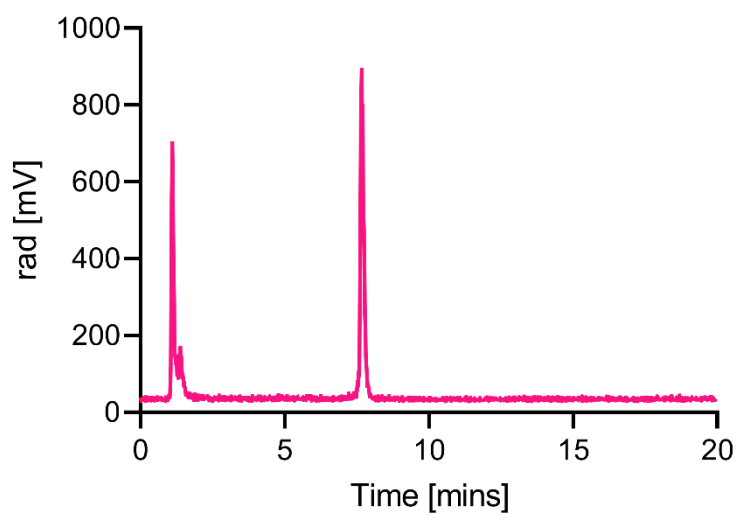


Figure S43. Radio-HPLC chromatogram of ^{68}Ga -PSMA-617 conducted on non-fractionated, buffered generator eluate.

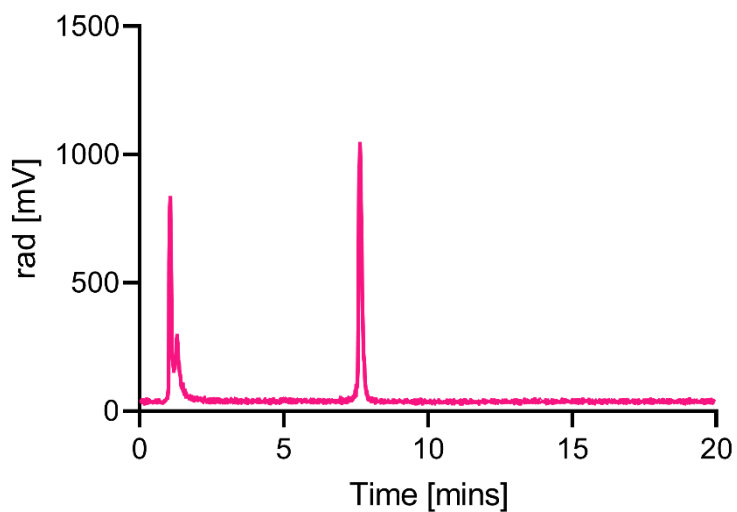


Figure S44. Radio-HPLC chromatogram of ^{68}Ga -PSMA-617 conducted on fractionated, buffered generator eluate.

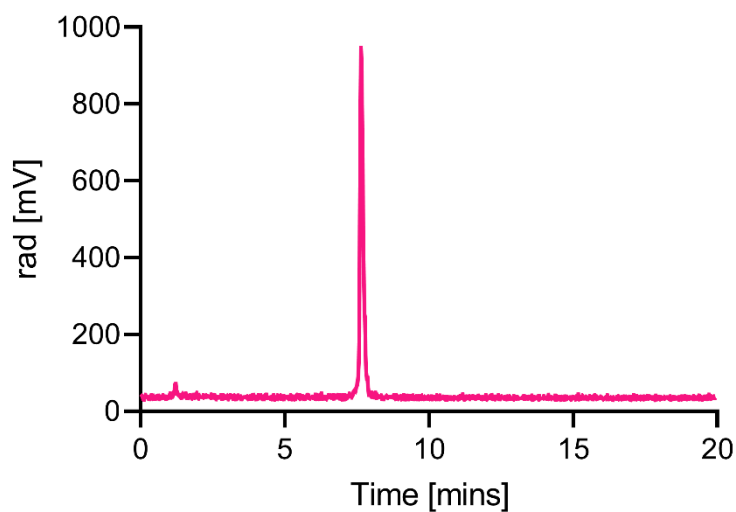


Figure S45. Radio-HPLC chromatogram of ^{68}Ga -31 conducted on non-fractionated, buffered generator eluate.

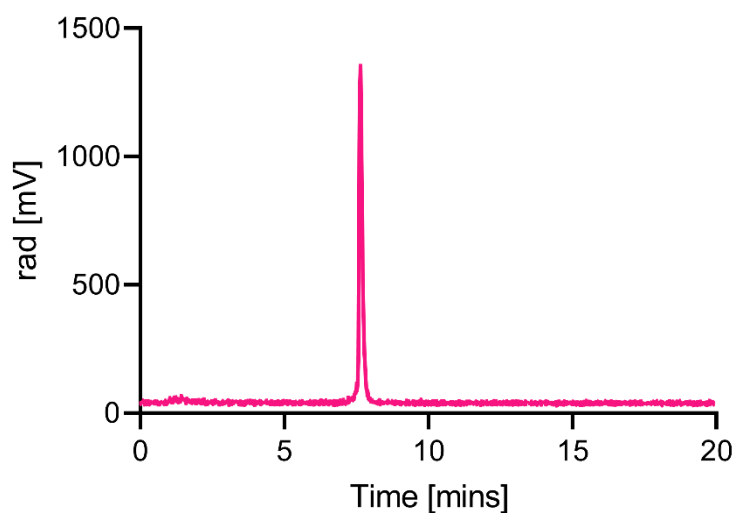


Figure S46. Radio-HPLC chromatogram of $^{68}\text{Ga-31}$ conducted on fractionated, buffered generator eluate.

6. Tabulated data.

Table S3. Photocleavage yields for 10 min for variable of LED/photon source to reaction vessel distances for 20 minute reaction time.

Distance LED-resin [mm]	PCY [%] (n=3)
1	50.00 ± 1.73
3	48.00 ± 2.00
5	44.00 ± 3.61
11	35.33 ± 4.04
21	16.67 ± 0.58

Table S4. Radiolabeling and photocleavage yields for the synthesis of $^{67}\text{Ga-10}$ using 10 nmol tentagel resin.

Time [min]	RCY [%] (n=3)	PCY [%] (n=3)
0	3.83 ± 1.31	N/A
10	82.00 ± 2.83	24.10 ± 2.30
20	87.50 ± 1.22	45.43 ± 1.38
30	90.33 ± 0.47	60.33 ± 0.47

Table S5. Radiolabeling and photocleavage yields for the synthesis of ⁶⁷Ga-10 using agarose resin.

Time [min]	RCY [%] (n=3)	PCY [%] (n=3)
0	3.83 ± 0.24	N/A
10	82.93 ± 2.85	21.03 ± 2.21
20	86.17 ± 1.65	40.90 ± 1.64
30	90.33 ± 1.25	49.67 ± 1.25

Table S6. Radiolabeling and photocleavage yields for the synthesis of ⁶⁷Ga-10 using ion-exchange resin.

Time [min]	RCY [%] (n=3)	PCY [%] (n=3)
0	3.17 ± 0.62	N/A
10	82.00 ± 1.63	11.40 ± 2.59
20	84.67 ± 0.47	17.37 ± 1.24
30	87.00 ± 0.82	25.00 ± 0.82

Table S7. Quantification of NOTA-containing conjugate in cleavage fractions. Amount of resin used: 0.1 mg (Loading: 0.16 mmol/g resin).

Photocleavage time [min]	Isolated 19 ligand [nmol] (n=3)
10	2.50 ± 0.50 (15%)
20	5.10 ± 1.20 (31%)
30	6.20 ± 0.84 (38%)
TFA cleavage, 30 min	15.4 ± 0.19 (96 %)

Table S8. Radiolabeling and photocleavage yields for the synthesis of ⁶⁷Ga-19 in presence of increasing amounts of cold ^{nat}Zn carrier.

Equivalent excess of cold ^{nat}Zn carrier (1 eq = 0.00125 nmol)	RCY [%] (n=3)	PCY [%] (n=3)
1	91.67 ± 0.58	36.00 ± 1.00
10	90.67 ± 0.58	34.33 ± 3.79
100	91.33 ± 1.15	38.67 ± 0.58
200	91.67 ± 1.53	40.00 ± 1.00
300	91.67 ± 0.58	38.33 ± 0.58
500	91.00 ± 1.00	39.67 ± 0.58
1000	91.33 ± 2.08	37.00 ± 2.65
10000	92.33 ± 1.53	38.33 ± 0.58
20000	90.67 ± 0.58	39.33 ± 1.53
30000	64.00 ± 1.73	35.00 ± 1.00

Table S9. ICP-OES data for the post-radiolabeling fraction and photocleavage fraction for the synthesis of ⁶⁷Ga-19 in presence of increasing amounts of cold ^{nat}Zn carrier.

Equivalent excess of cold ^{nat}Zn carrier (1 eq = 0.00125 nmol)	^{nat}Zn carrier [%] in post-radiolabeling fraction (n=3)	^{nat}Zn carrier [%] in photocleavage fraction (n=3)
300	99.67 ± 0.80	0.33 ± 0.18
500	99.00 ± 1.10	1.00 ± 0.36
1000	99.33 ± 1.98	0.67 ± 0.22
10000	99.13 ± 1.13	0.87 ± 0.38
20000	98.67 ± 0.98	1.33 ± 0.34
30000	33.10 ± 1.62	66.90 ± 1.50

Table S10. Radiolabeling and photocleavage yields for the synthesis of $^{64}\text{Cu-19}$ in presence of increasing amounts of cold $^{\text{nat}}\text{Ni}$ carrier.

Equivalent excess of cold $^{\text{nat}}\text{Ni}$ carrier (1 eq = 0.1 pmol)	RCY [%] (n=3)	PCY [%] (n=3)
1	91.33 ± 1.15	36.67 ± 2.89
10	92.00 ± 1.73	38.33 ± 2.31
100	92.33 ± 1.15	37.67 ± 0.58
10000	92.33 ± 0.58	37.33 ± 2.89
12000	45.33 ± 1.53	32.33 ± 3.06

Table S11. Non-decay-corrected, radiochemical yield (RCY) and radiochemical purity (RCP) for the synthesis of $^{68}\text{Ga-31}$.

Eluate	RCY [%] (n=3)	RCP [%] (n=3)
A (diluted)	50.33 ± 2.05	90.00 ± 4.08
B (undiluted)	52.67 ± 2.49	94.00 ± 3.27

Table S12. Non-decay-corrected, radiochemical yield (RCY) and radiochemical purity (RCP) for the synthesis of $^{68}\text{Ga-PSMA-617}$.

Eluate	RCY [%] (n=3)	RCP [%] (n=3)
A (diluted)	22.33 ± 2.05	62.67 ± 4.11
B (undiluted)	32.33 ± 2.05	72.67 ± 2.05

Table S13. Cell binding data

Cell type	⁶⁸Ga-31 [%] (n=3)	⁶⁸Ga-PSMA-617 [%] (n=3)
PC3 PiP	19.57 ± 1.38	16.45 ± 0.63
PC3 Flu	0.60 ± 0.09	0.38 ± 0.10

Table S14. Decay-corrected biodistribution of ⁶⁸Ga-31 90 min post- injection (n=6)

Organ	⁶⁸Ga-31 90 min (n=6)
Blood	0.14 ± 0.0007
Heart	0.12 ± 0.0001
Lung	0.31 ± 0.0012
Liver	0.35 ± 0.0011
Spleen	0.19 ± 0.0005
Kidney	1.66 ± 0.0062
Sm Int	0.15 ± 0.0006
Muscle	0.12 ± 0.0005
Bone	0.12 ± 0.0003
PSMA + Tumor	10.33 ± 0.0492
PSMA - Tumor	0.48 ± 0.0016

7. References

1. Lampkin, P. P.; Thompson, B. J.; Gellman, S. H., Versatile Open-Source Photoreactor Architecture for Photocatalysis Across the Visible Spectrum. *Org. Lett.* **2021**, *23* (13), 5277-5281.
2. Abd-Elgaliel, W. R.; Gallazzi, F.; Lever, S. Z., Total solid-phase synthesis of bombesin analogs with different functional groups at the C-terminus. *J. Pept. Sci.* **2007**, *13* (7), 487-492.
3. Vaughn, B. A.; Loveless, C. S.; Cingoranelli, S. J.; Schlyer, D.; Lapi, S. E.; Boros, E. J. M. p., Evaluation of ¹⁷⁷Lu and ⁴⁷Sc Picaga-Linked, Prostate-Specific Membrane Antigen-Targeting Constructs for Their Radiotherapeutic Efficacy and Dosimetry. **2021**, *18* (12), 4511-4519.
4. Hackenberger, C. P., The reduction of oxidized methionine residues in peptide thioesters with NH₄I–Me₂S. *Org. Biomol. Chem.* **2006**, *4* (11), 2291-2295.
5. Lee, L. L.; Buckton, L. K.; McAlpine, S. R., Converting polar cyclic peptides into membrane permeable molecules using N-methylation. *J. Pept. Sci.* **2018**, *110* (3), e24063.
6. Pandey, A.; Smilowicz, D.; Boros, E., Galbofloxacin: a xenometal-antibiotic with potent in vitro and in vivo efficacy against *S. aureus*. *Chem Sci* **2021**, *12* (43), 14546-14556.